

Near-Infrared Photometry of Carbon Stars^{*}

Patricia A. Whitelock^{1,2,3,†}, Michael W. Feast², Freddy Marang¹ and M.A.T. Groenewegen⁴

¹ South African Astronomical Observatory, P.O.Box 9, 7935 Observatory, South Africa

² Astronomy Department, University of Cape Town, 7701 Rondebosch, South Africa

³ National Astrophysics and Space Science Programme, University of Cape Town, 7701 Rondebosch, South Africa

⁴ Instituut voor Sterrenkunde, KU Leuven, Celestijnenlaan 200B, B-3001 Leuven, Belgium

Received date; accepted date

ABSTRACT

Near-infrared, *JHKL*, photometry of 239 Galactic carbon-rich variable stars is presented and discussed. From these and published data the stars were classified as Mira or non-Mira variables and amplitudes and pulsation periods, ranging from 222 to 948 days for the Miras, were determined for most of them. A comparison of the colour and period relations with those of similar stars in the Large Magellanic Cloud indicates minor differences, which may be the consequence of sample selection effects. Apparent bolometric magnitudes were determined by combining the mean *JHKL* fluxes with mid-infrared photometry from IRAS and MSX. Then, using the Mira period luminosity relation to set the absolute magnitudes, distances were determined – to greater accuracy than has hitherto been possible for this type of star. Bolometric corrections to the *K* magnitude were calculated and prescriptions derived for calculating these from various colours. Mass-loss rates were also calculated and compared to values in the literature.

Approximately one third of the C-rich Miras and an unknown fraction of the non-Miras exhibit apparently random obscuration events that are reminiscent of the phenomena exhibited by the hydrogen deficient RCB stars. The underlying cause of this is unclear, but it may be that mass loss, and consequently dust formation, is very easily triggered from these very extended atmospheres.

Key words: stars: individual: EV Eri, R Lep, R Vol, IRAS09164–5349, IRAS10136–5743, IRAS16406–1406 - stars: variable: other - dust, extinction - infrared: stars - stars: carbon - stars: AGB and post-AGB - stars: distances.

1 INTRODUCTION

Intrinsic carbon stars are produced when asymptotic giant branch (AGB) stars experience sufficient dredge-up to change their surface carbon to oxygen ratios from $C/O < 1$ to $C/O > 1$. Exactly how and when this occurs depend on the initial mass and the abundances of the star in question, but the details remain controversial. It has been known for a long while that the majority of the C stars in the Magellanic Clouds were low mass objects (e.g. Iben 1981), but it has only recently been possible to model the production of C stars among relatively low mass stars (e.g. Stancliffe et al. 2005).

In attempting to find an appropriate group of local C stars to study it is natural to examine the large amplitude

variables. First, the amplitude of their variability identifies them as AGB stars and therefore one can be reasonably certain that their carbon enrichment is intrinsic rather than the result of binary mass transfer. Secondly, observations of extragalactic C Miras suggest that they obey a well defined period luminosity relation (Feast et al. 1989, Whitelock et al. 2003) and it should therefore be possible to establish their distances, provided their periods and apparent luminosities can be measured.

This particular project arose from the requirement to identify a significant local population of Galactic C stars with distances and radial velocities which could be used for kinematic studies. From these it should be possible to gain insight into the nature, in particular the ages and masses, of the local C star population which will be invaluable for comparison with theory and with similar populations in Local Group galaxies (e.g. Menzies et al. 2002).

In this paper, the first of three, we discuss infrared pho-

^{*} This paper is based on observations made at the South African Astronomical Observatory.

[†] e-mail: paw@sao.ac.za

tometry of C variables observable from the southern hemisphere. Subsequent papers will deal with radial velocities and northern C-rich Miras (Menziés et al. 2006, Paper II) and the kinematics of the full sample (Feast et al. 2006, Paper III).

2 SOURCE SELECTION

Much of the *JHKL* photometry reported here comes from two specific programmes; first, stars selected from the catalogue of Aaronson et al. (1989) and secondly, stars selected from the IRAS Point Source Catalogue (IRAS Science Team 1985), henceforth referred to as the ‘Aaronson’ and ‘IRAS’ samples, respectively. The stars from each group were monitored for several years to determine their pulsation periods and to establish the characteristics of their variability. These data were supplemented by observations of C stars that had been obtained from SAAO over the years as part of other programmes. In general stars were selected to be south of declination $+30^\circ$ for ease of monitoring from Sutherland.

Aaronson et al. (1989) published velocities and *JHK* photometry for C stars. The stars selected for monitoring were chosen on the basis of their colours ($(H - K)_0 > 0.8$) (using a very rough estimate of the reddening correction) or their *K* variability as potential Mira variables which could be used to establish the kinematic properties of the C Miras (the colour criterion may have resulted in the omission of some C Miras, but the objective was to find stars with a high probability of being C Miras rather than to be complete). These stars are identified with an ‘A’ in column 10 (G) of Table 1. Data are reported here for 60 such stars, including three which are probably not C stars.

The IRAS sample was selected from the Point Source Catalogue (PSC) using the following 3 criteria: spectral types 4n, indicating SiC features in the LRS spectra; 25 to 12 μm flux ratio, $F_{25}/F_{12} > 0.4$; 12 μm flux, $F_{12} > 40$ Jy. The flux ratio criterion was intended to isolate stars with dust shells; while the limit to the 12 μm flux was intended to ensure that the stars would be observable, at least at *K* and *L*, on the 0.75m at Sutherland. Note that the spectral-type criterion will have resulted in the omission of C Miras without SiC shells, but again the objective was to find stars with a high probability of being C-rich Miras rather than to be complete. Some of the stars selected in this way were already being observed as part of other programmes; nevertheless, they will be identified as part of the ‘IRAS’ sample for the purpose of the discussion below. These stars are identified with an ‘I’ in column 10 (G) of Table 1. Data are presented for 96 such IRAS sources, including five which are unlikely to be C stars.

A further 32 C-stars with IRAS photometry have $F_{25}/F_{12} > 0.4$, but with $F_{12} < 40$. These were not chosen on the basis of their IRAS characteristics but are identified here with an ‘i’ in column 10 (G) as an interesting group to compare with their brighter counterparts. Five of the stars selected in this way are probably not C stars.

A number of sources from the Aaronson and IRAS samples were identified by the selection criteria mentioned above, but observations proved impossible because of severe crowding.

There are only two stars in common between the Aaron-

son and the IRAS samples, although another 8 are found in the faint IRAS sample. This might suggest that the fainter IRAS sources are not simply more distant but that they actually have thinner shells than their brighter counterparts.

The names of the C stars are listed in Table 1 in one of the forms recognizable by the SIMBAD data base, with preference being given to a variable star designation (from Samus et al. 2004, henceforth GCVS) where one exists. IRAS names are also listed, and are used throughout this paper without the ‘IRAS’ prefix. The C numbers listed in the table are from the updated version of Stephenson’s Catalogue of Galactic Carbon Stars (Alksnis et al. 2001). Most of the coordinates were taken from Cutri et al. (2003, henceforth 2MASS).

At the end of Table 1 18 stars are listed which were observed as part of the programme, but which are either peculiar in some way or are probably not bona fide C stars. Peculiarities include transitional objects, i.e. SC stars.

3 INFRARED PHOTOMETRY

The detailed SAAO photometry is reported in Table 3 for the first star only, the full dataset of photometry is available electronically. The table gives times of the observations as Julian Date (JD) followed by the *JHKL* mags measured for that date. It is organized in order of right ascension with the dubious C stars (the 18 listed at the end of Table 1) mixed among the definite ones. Where measurements were not made, usually at *J* or *L* because the star was too faint, the column is left blank. Most of the *JHKL* measurements were made with the MkII infrared photometer on the 0.75-m telescope at SAAO, Sutherland. They are on the current SAAO system as defined by Carter (1990). A few measurements were made on the SAAO 1.9-m and these have been transformed to the SAAO system¹. These are marked ‘1.9m’ in the last column of the table.

The post-1979 photometry is accurate to better than ± 0.03 mag at *JHK*, and to better than ± 0.05 mag at *L*; observations with $J > 13.0$, measured using the 1.9m telescope, or $J > 10.4$ measured using the 0.75m, are good to ± 0.06 at *J*. Measurements marked with a colon are accurate to better than 0.1 mag. Some older (pre-1979) measurements were reported by Catchpole et al. (1979). The measurements listed here differ slightly from those in Catchpole et al., because they have been corrected to Carter’s improved values for the standard stars. These measurements are slightly less accurate than the more modern values, but see Catchpole et al. for details.

¹ Transformation from the 1.9-m natural system to the SAAO system defined by Carter (1990) assumes $K_{1.9} = K$ and $(J - H)_{1.9} = 0.95(J - H)$ or $(J - K)_{1.9} = 0.955(J - K)$.

Table 1: Stars observed in this survey.

name	IRAS	RA		Dec			MSX	G	C	comment
Equinox 2000										
R Scl	01246-3248	1	26	58	-32	32	36		I	234
YY Tri	02152+2822	2	18	6	+28	36	45		I	6028
R For	02270-2619	2	29	15	-26	5	56			361
EV Eri	04067-0922	4	9	6	-9	14	12		i	6070
[TI98]0418+0122	04188+0122	4	21	27	+1	29	14			6075
V718 Tau	04284+1732	4	31	22	+17	39	10			714
TT Tau	04483+2826	4	51	31	+28	31	37			794
R Lep	04573-1452	4	59	36	-14	48	23			833
TU Tau	05421+2424	5	45	14	+24	25	12	X		1038
Y Tau	05426+2040	5	45	39	+20	41	42			1042
QS Ori	05428+1215	5	45	37	+12	16	15			395
05418-3224	05418-3224	5	43	43	-32	23	29		I	1045
V1259 Ori	06012+0726	6	4	00	+7	25	52		I	6113
06088+1909	06088+1909	6	11	48	+19	8	20	X	I	1187
BN Mon	06192+0722	6	21	58	+7	20	58	X		1246
ZZ Gem	06209+2503	6	24	01	+25	1	53			1251
V617 Mon	06210+0831	6	23	48	+8	29	51	X		1254
V636 Mon	06226-0905	6	25	1	-9	7	16			6146
V477 Mon	06268+0849	6	29	35	+8	47	16	X	I	1287
CR Gem	06315+1606	6	34	24	+16	4	30	X	i	1309
GM CMa	06391-2213	6	41	15	-22	16	43		i	1357
V503 Mon	06422+0953	6	44	57	+9	50	48	X		1377
RT Gem	06436+1840	6	46	35	+18	36	54			1389
06487+0551	06487+0551	6	51	24	+5	47	34	X	I	1430
CG Mon	06487+0517	6	51	27	+5	13	23	X		1431
CL Mon	06529+0626	6	55	37	+6	22	43			1465
06531-0216	06531-0216	6	55	40	-2	20	16	X		1471
NP Pup	06528-4218	6	54	27	-42	21	56			1478
06564+0342	06564+0342	6	59	6	+3	37	56	X	I	1494
W CMa	07057-1150	7	8	3	-11	55	24	X	i	1565
07080-0106	07080-0106	7	10	35	-1	11	26		I	1580
VX Gem	07099+1441	7	12	49	+14	36	4			1595
07097-1011	07097-1011	7	12	8	-10	16	39	X	A	1597
R Vol	07065-7256	7	5	36	-73	0	52			1599
HX CMa	07098-2012	7	12	4	-20	17	23		I	1601
07136-1512	07136-1512	7	15	57	-15	18	08	X	A	1630
07161-0111	07161-0111	7	18	39	-1	16	52		I	1642
07217-1246	07217-1246	7	24	3	-12	52	28	X	AI	1696
07220-2324	07220-2324	7	24	7	-23	30	46		I	1699
07223-1553	07223-1553	7	24	35	-15	59	52	X	A	1701
07293-1832	07293-1832	7	31	31	-18	39	4	X	A	1751
07319-1940	07319-1940	7	34	6	-19	46	56	X	A	1775
[W71b]W007-02	07348-1926	7	37	2	-19	32	54	X	A	1798
07373-4021	07373-4021	7	39	4	-40	28	47			1825
[W71b]W008-03		7	40	55	-26	1	31	X	A	1831
V471 Pup	07390-2618	7	41	6	-26	25	19	X	A	1834
[ABC89]Pup 3	07403-2943	7	42	17	-29	51	4	X	Ai	1847
[ABC89]Pup 17		7	49	32	-27	23	36	X	A	1897
07454-7112	07454-7112	7	45	2	-71	19	46		I	1901
[ABC89]Pup 21	07506-2819	7	52	43	-28	26	52	X	A	1924
V831 Mon	07551-0032	7	57	43	-0	41	6			1960
07576-4054	07576-4054	7	59	24	-41	3	16		I	1992
07582-1933	07582-1933	8	0	25	-19	42	11		I	1993
V509 Pup	08004-3023	8	2	26	-30	32	16	X	A	2010
[ABC89]Pup 38	08010-2626	8	3	7	-26	34	31	X	A	6268
FF Pup	08014-2356	8	3	35	-24	4	35			2022
[ABC89]Pup 42	08029-2942	8	4	58	-29	51	26	X	A	2043

Continued on Next Page...

name	IRAS	RA						Dec	MSX	G	C	comment
		Equinox 2000										
V518 Pup	08045-1524	8	6	51	-15	33	23		I	2056		
08050-2838	08050-2838	8	7	6	-28	47	40	X	I	2062		
RU Pup	08053-2246	8	7	30	-22	54	45			2064		
FK Pup	08073-3608	8	9	11	-36	17	7	X		2086		
08074-3615	08074-3615	8	9	20	-36	24	27	X	I	6267		
[ABC89]Ppx19	08080-3259	8	10	2	-33	8	29	X	A	2091		
[W71b]021-05	08083-3145	8	10	18	-31	54	22	X	A	2095		
[ABC89]Ppx22	08085-3351	8	10	29	-34	0	36	X	A	2099		
V346 Pup	08088-3243	8	10	49	-32	52	6	X	AI	2101		
[W71b]026-01	08160-3822	8	17	52	-38	32	16	X	A	2146		
RY Hya	08174+0255	8	20	6	+2	45	56			2150		
[ABC89]Ppx40	08197-3447	8	21	41	-34	57	24	X	A	2173		
[W71b]029-02	08233-4110	8	25	10	-41	20	2	X	A	2203		
[W71b]029-04	08266-4110	8	28	26	-41	20	43	X	A	2224		
08340-3357	08340-3357	8	36	3	-34	7	34		I	2260		
R Pyx	08434-2801	8	45	31	-28	12	3			2326		
UW Pyx	08450-3407	8	47	00	-34	18	59			2334		
T Cnc	08538+2002	8	56	40	+19	50	57			2384		
08535-4724	08535-4724	8	55	11	-47	35	56	X	I	2389		
08534-5055	08534-5055	8	55	2	-51	7	20	X	I	2390		
IQ Hya	09112-2311	9	13	32	-23	23	31			2450		
CQ Pyx	09116-2439	9	13	54	-24	51	25		I	6325		
09164-5349	09164-5349	9	18	2	-54	2	27	X	I	2473		
09176-5147	09176-5147	9	19	17	-52	0	28	X	I	2476		
[ABC89]Vel19		9	26	19	-52	6	4	X	A	2508		
[W71b]046-02	09249-4909	9	26	45	-49	22	25	X	A	2512		
[ABC89]Vel44	09331-5010	9	34	57	-50	24	30	X	A	2563		
09433-6233	09433-6233	9	44	41	-62	47	32		i	6339		
CW Leo	09452+1330	9	47	57	+13	16	43		I	2619		
W Sex	09484-0147	9	50	58	-2	1	43			2635		
09484-6242	09484-6242	9	49	49	-62	56	9			2645		
09513-5324	09513-5324	9	53	7	-53	38	54	X	I	2653		
09529-5506	09529-5506	9	54	41	-55	20	16	X	I	2660		
09533-6021	09533-6021	9	54	52	-60	35	26		i	2663		
09521-7508	09521-7508	9	52	30	-75	22	28		I	2664		
09586-6150	09586-6150	10	0	9	-62	5	19		i	6344		
10019-6156	10019-6156	10	3	29	-62	10	37			2691		
10023-5946	10023-5946	10	3	58	-60	0	37	X		2692		
10026-5849	10026-5849	10	4	20	-59	4	0	X		6347		
10052-5906	10052-5906	10	6	57	-59	21	25	X		2703		
10098-5742	10098-5742	10	11	35	-57	57	53	X	i	6352		
10109-5958	10109-5958	10	12	40	-60	13	30	X		2720		
RW LMi	10131+3049	10	16	2	+30	34	19			2724		
10130-5703	10130-5703	10	14	49	-57	18	45	X	i			
10136-5743	10136-5743	10	15	27	-57	58	11	X		2729		
10145-6046	10145-6046	10	16	13	-61	1	43			2734		
10149-5919	10149-5919	10	16	43	-59	34	52	X		2735		
10151-6008	10151-6008	10	16	50	-60	23	55	X	i	6354		
10175-5957	10175-5957	10	19	17	-60	12	52	X		2745		
10199-5801	10199-5801	10	21	44	-58	16	35	X	i	6363		
10220-5858	10220-5858	10	23	49	-59	13	54	X		6366		
CPD-58 2175	10231-5823	10	24	58	-58	39	17	X	i	2760		
CZ Hya	10249-2517	10	27	18	-25	32	56			2764		
[ABC89]Car5		10	29	44	-62	28	29		A	2776		
[ABC89]Car11		10	32	22	-60	42	29	X	A	2784		
TV Vel	10324-5358	10	34	28	-54	14	28			2790		
U Ant	10329-3918	10	35	13	-39	33	45			2793		
[ABC89]Car28		10	37	9	-60	59	34	X	A	6391		
[ABC89]Car32	10366-5950	10	38	29	-60	5	57	X	A	2817		

Continued on Next Page...

name	IRAS	RA						MSX	G	C	comment
		Equinox 2000									
FU Car	10390-5907	10	41	0	-59	23	13	X	Ai	2832	
[ABC89]Car54	10442-5809	10	46	16	-58	25	21	X	A	2850	
[ABC89]Car59		10	48	30	-60	11	32	X	A	2862	
V Hya	10491-2059	10	51	37	-21	15	00		I	2877	
[ABC89]Car73	10509-6036	10	52	55	-60	52	10	X	A	6426	
[ABC89]Car81		10	54	27	-60	19	50	X	A	2897	
[ABC89]Car84		10	56	45	-60	3	37	X	A	2907	
[ABC89]Car87	10558-6203	10	57	47	-62	19	16	X	A	2911	
[ABC89]Car93		10	59	5	-60	31	49		A	2917	
[ABC89]Car105	11009-6117	11	3	1	-61	33	28	X	Ai	2941	
11145-6534	11145-6534	11	16	39	-65	50	56		I	2987	
[W65] c1		11	20	34	-59	30	51	X		2997	
[W65] c2		11	22	5	-59	38	45	X	A	3003	
[W65] c13	11299-6103	11	32	19	-61	20	34	X	A	3051	
[TI98]1130-1020	11308-1020	11	33	25	-10	36	59			3052	
11318-7256	11318-7256	11	33	58	-73	13	19			3062	
[ABC89]Cen3		11	35	54	-60	33	41	X	A	3068	
[ABC89]Cen4	11339-6012	11	36	17	-60	29	18	X	A	3071	
11463-6320	11463-6320	11	48	48	-63	37	28	X	I	6455	
[ABC89]Cen32	11468-5950	11	49	21	-60	7	5	X	Ai	3108	
[ABC89]Cen43	11510-6046	11	53	31	-61	3	33	X	A	3120	
[ABC89]Cen60	11556-6357	11	58	8	-64	14	54	X	A	3139	
[ABC89]Cen78		12	4	10	-62	42	26	X	A	6464	
CF Cru	12023-6230	12	4	55	-62	47	39	X	A	3165	
[ABC89]Cen97	12100-6122	12	12	44	-61	39	01	X	A	6473	
12194-6007	12194-6007	12	22	10	-60	24	15	X	I	3220	
SS Vir	12226+0102	12	25	14	+ 0	46	11			3236	
12298-5754	12298-5754	12	32	41	-58	11	29	X	I	3251	
CGCS3268	12374-5706	12	40	15	-57	22	46		A	3268	
12394-4338	12394-4338	12	42	10	-43	55	03		I	3275	
12421-6217	12421-6217	12	45	7	-62	33	38	X	I	6489	
RU Vir	12447+0425	12	47	18	+ 4	8	41			3286	
V Cru	12536-5737	12	56	36	-57	53	57	X		3310	
12540-6845	12540-6845	12	57	16	-69	1	51		I	3311	
[ABC89]Cru17	13022-6400	13	5	26	-64	16	11	X	Ai	3327	
[ABC89]Cir1	13342-6232	13	37	44	-62	48	28	X	Ai	3410	
13343-5807	13343-5807	13	37	41	-58	23	10	X	I	3411	
13477-6532	13477-6532	13	51	29	-65	46	56	X	I	3439	
13482-6716	13482-6716	13	52	4	-67	30	56		I	3441	
13509-6348	13509-6348	13	54	34	-64	3	23	X	I	3446	
[ABC89]Cir18		13	55	26	-59	22	24	X	A	6547	
[ABC89]Cir26	14004-6047	14	4	5	-61	01	50	X	Ai	6549	
[ABC89]Cir27	14010-5927	14	4	33	-59	41	22	X	Ai	3470	
[W71b]093-02	14192-6327	14	23	8	-63	41	9	X	A	3487	
14395-5656	14395-5656	14	43	14	-57	8	45	X	A	3523	
14404-6320	14404-6320	14	44	26	-63	33	28	X	I	3525	
14443-5708	14443-5708	14	48	4	-57	20	37	X	I	6565	
15082-4808	15082-4808	15	11	41	-48	19	59		I	3570	
15084-5702	15084-5702	15	12	15	-57	13	28	X	I	6572	
II Lup	15194-5115	15	23	5	-51	25	59	X	I	3592	
15261-5702	15261-5702	15	30	2	-57	12	46	X	I		
15471-5644	15471-5644	15	51	6	-56	53	24	X	I	6600	
CGCS3660		16	2	44	-41	21	32			3660	
16079-4812	16079-4812	16	11	34	-48	19	51	X	I	3670	
NP Her	16150+2558	16	17	9	+25	51	02			3679	
16171-4759	16171-4759	16	20	50	-48	6	53	X	I	3681	
V Oph	16239-1218	16	26	44	-12	25	36			3698	
SU Sco	16374-3217	16	40	39	-32	22	48			3720	
CGCS3721	16387-5401	16	42	45	-54	7	10			3721	

Continued on Next Page...

name	IRAS	RA						Dec	MSX	G	C	comment
		Equinox 2000										
16406-1406	16406-1406	16	43	27	-14	12	00			i		
16538-4633	16538-4633	16	57	32	-46	37	47	X		I	3747	
16545-4214	16545-4214	16	58	6	-42	19	24	X		I	3748	
T Ara	16584-5459	17	2	33	-55	4	16			i	3756	2
V901 Sco	16595-3239	17	2	46	-32	43	31	X			3762	
17047-2848	17047-2848	17	7	56	-28	52	06			I	3772	
V2548 Oph	17049-2440	17	7	58	-24	44	31			I	6661	
SZ Ara	17065-6153	17	11	7	-61	57	15				3774	
V617 Sco	17103-3551	17	13	41	-35	55	21	X		I	3786	
17105-3746	17105-3746	17	13	59	-37	50	8	X		I	6670	3
17130-3907	17130-3907	17	16	33	-39	10	46	X		I	3794	
17209-3318	17209-3318	17	24	15	-33	21	20	X		I	6674	4
17217-3916	17217-3916	17	25	13	-39	19	22	X		I	3823	
17222-2328	17222-2328	17	25	18	-23	30	46			I	3825	
V833 Her	17297+1747	17	31	55	+17	45	21			I	6677	
V Pav	17389-5742	17	43	19	-57	43	26				3861	
17446-4048	17446-4048	17	48	12	-40	49	36			I	6685	
17446-7809	17446-7809	17	52	35	-78	10	42			I	6687	
17463-4007	17463-4007	17	49	50	-40	7	58					5
V348 Sco	17478-4315	17	51	30	-43	16	23			i	3886	
17581-1744	17581-1744	18	1	6	-17	44	23	X		I	3925	
18036-2344	18036-2344	18	6	42	-23	44	22	X		I	6709	
FX Ser	18040-0941	18	6	50	-9	41	16			I	6711	
V1280 Sgr	18073-2652	18	10	28	-26	51	58	X			3960	
18119-2244	18119-2244	18	15	1	-22	43	58	X		I	6729	
18147-2215	18147-2215	18	17	43	-22	14	39	X		I	6733	
V5104 Sgr	18194-2708	18	22	35	-27	6	29				6738	
V2548 Sgr	18234-2206	18	26	29	-22	4	15	X		I	4007	
18239-0655	18239-0655	18	26	39	-6	54	4	X		I	6743	
18244-0815	18244-0815	18	27	7	-8	13	10	X		i		
V1076 Her	18240+2326	18	25	6	+23	28	47			I		
18248-0839	18248-0839	18	27	34	-8	37	23	X		I	4014	
18269-1257	18269-1257	18	29	47	-12	54	58	X		I	4024	
18320-0352	18320-0352	18	34	40	-3	50	14	X		I	6750	
V627 Oph	18321+0910	18	34	34	+9	12	42				4045	
18367-0452	18367-0452	18	39	22	-4	48	45	X		I	6754	3
V1417 Aql	18398-0220	18	42	25	-2	17	27	X		I	4077	
18400-0704	18400-0704	18	42	45	-7	1	10	X		i	6757	
V821 Her	18397+1738	18	41	55	+17	41	8			I	4078	
18424+0346	18424+0346	18	44	59	+3	49	35	X		I	4093	
V874 Aql		18	45	41	+9	38	39				4099	
V2045 Sgr	18463-1706	18	49	15	-17	3	25				4117	
S Sct	18476-0758	18	50	20	-7	54	28	X			4121	
18475+0926	18475+0926	18	49	55	+9	30	07	X		I	6761	
AI Sct	18481-0647	18	50	52	-6	44	23	X			4124	
V1418 Aql	19008+0726	19	3	18	+7	30	45	X		I	4162	
19029+2017	19029+2017	19	5	7	+20	22	4			I	6767	
19068+0544	19068+0544	19	9	16	+5	49	10	X		I	6772	
V1420 Aql	19175-0807	19	20	18	-8	2	12			I	6780	
V374 Aql	19276-0056	19	30	15	-0	50	9			I	4301	
V1965 Cyg	19321+2757	19	34	10	+28	4	8	X		I	4347	
19358+0917	19358+0917	19	38	13	+9	24	9			I	4378	
19455+0920	19455+0920	19	47	56	+9	28	9			I	4475	
R Cap	20084-1425	20	11	18	-14	16	3				4701	
RT Cap	20141-2128	20	17	7	-21	19	4				4774	
BD Vul	20351+2618	20	37	18	+26	29	13				4915	
V442 Vul	20570+2714	20	59	10	+27	26	39			I	5063	
RV Aqr	21032-0024	21	5	52	-0	12	42				5120	
Y Pav	21197-6956	21	24	17	-69	44	2				5239	

Continued on Next Page...

name	IRAS	RA		Dec			MSX	G	C	comment	
Equinox 2000											
[TI98]2223+2548	22239+2548	22	26	19	+26	3	38				
[TI98]2259+1249	22592+1249	23	1	47	+13	5	14				
LL Peg	23166+1655	23	19	13	+17	11	33	I	6913		
RU Aqr	23217-1735	23	24	24	-17	19	9	i			
IZ Peg	23257+1038	23	28	17	+10	54	37	I	6916		
CS stars, peculiar and uncertain C stars											
R Ori	04562+0803	4	58	59	+ 8	7	49		828	6	
R CMi	07059+1006	7	8	42	+10	1	26		1561	6	
08276-5125	08276-5125	8	29	8	-51	35	5	i		C?	
08439-2734	08439-2734	8	46	6	-27	45	49	I	2329	7	
UX Pyx	09075-2758	9	9	41	-28	10	21	i		8	
MU Vel	09450-4716	9	46	54	-47	29	51	i		C?	
10226-5229	10226-5229	10	24	34	-52	43	29	I		C?	
[ABC89]Car10	10293-5912	10	31	9	-59	28	16	X	Ai	6382	9
TU Car	10331-6027	10	34	55	-60	42	35	X	A	2795	10
V354 Cen		11	50	59	-47	55	21				C?
[ABC89]Cen50	11529-6350	11	55	29	-64	7	23	X	A		9
BH Cru	12135-5600	12	16	16	-56	17	7				6
TT Cen	13163-6031	13	19	34	-60	46	44	X	i	3367	6
RV Cen	13343-5613	13	37	35	-56	28	33			3412	11
16316-5026	16316-5026	16	35	30	-50	32	10		I		8
VX Aql	18575-0139	19	0	9	- 1	34	56	X			6
18595-3947	18595-3947	19	3	2	-39	42	56		I		12
V1293 Aql	19306+0455	19	33	6	+ 5	1	45		I		13

Notes:

1. Complex flattened circumstellar shell (Richichi et al. 1998).
 2. Super lithium rich star (Catchpole & Feast 1976).
 3. No 2MASS photometry; image blended.
 4. C star 35'' east of OH353.81+1.45; IRAS probably blend of two.
 5. 17463-4007 is the only known cool C star in the Bulge as noted from an objective prism survey by S. Hughes (private communication).
 6. SC star (Keenan & Boeshaar 1980).
 7. SC star (Lloyd Evans 1991).
 8. SIMBAD quotes spectral type other than C.
 9. S star (Lloyd Evans & Catchpole 1989).
 10. Not a C star (Aaronson et al. 1989).
 11. C star with silicate shell (Skinner et al. 1990).
 12. Not a C star (Chen et al. 2003).
 13. Not a C star, e.g. Groenewegen (1994) and references therein.
- C? These have been suggested as C rich on the basis of their infrared colours or IRAS spectra, but the evidence is inconclusive.

Table 2: Near-infrared data.

Name	<i>J</i>	<i>H</i>	<i>K</i>	<i>L</i>	ΔJ	ΔH	ΔK	ΔL	P_K	P_{lit}	Var	no.	
				(mag)									
												(day)	
R Scl	2.02	0.66	-0.08	-0.73	0.86	0.64	0.36	0.28	375	363	20	157	
YY Tri		9.82	6.81	3.06		1.80	1.74	1.40	624		10	74	
R For	4.08	2.41	1.21	-0.07	1.10	0.92	0.66	0.58	385	389	11 [†]	100	
EV Eri	5.55	4.30	3.60	3.00					226		21 [†]	59	
[TI98]0418+0122	9.23	7.36	6.01	4.53	1.64	1.42	1.08	0.78	422		10	31	
V718 Tau	5.92	4.07	2.84	1.63	1.46	1.18	0.78	0.80	388	405	13*	14	
TT Tau	2.78	1.45	0.97	0.54						166	20	1	
R Lep	2.49	1.03	0.07	-0.94	0.94	0.78	0.52	0.50	438	427	11 [†]	71	

Continued on Next Page...

Name	<i>J</i>	<i>H</i>	<i>K</i>	<i>L</i>	ΔJ	ΔH	ΔK	ΔL	P_K	P_{lit}	Var	no.
TU Tau	3.62	2.25	1.68	1.09						190:	20	1
Y Tau	2.13	0.83	0.27	-0.29						242	20	6
QS Ori	6.40	4.82	3.80	2.73	1.58	1.44	1.02	1.00	483	476	10	12
05418-3224	9.15	6.68	4.86	2.75	1.70	1.56	1.36	1.30	483		11:*	15
V1259 Ori		11.29	7.73	3.44						696	10	2
06088+1909	8.57	6.07	4.26	2.25	1.38	1.20	1.00	0.86	493		10	13
BN Mon	4.44	2.99	2.24	1.59						600:	20	3
ZZ Gem	5.41	4.02	3.21	2.60	>0.8	>0.6	>0.4	>0.2	316:	317	10	9
V617 Mon	7.24	5.45	4.17	2.83	0.88	0.84	0.72	0.62	444	375:	14*	13
V636 Mon	5.01	3.13	1.82	0.41	1.62	1.26	0.86	0.56	543		10	15
V477 Mon	8.87	6.45	4.55	2.26	1.66	1.48	1.22	0.96	619	820:	10	12
CR Gem	3.36	1.91	1.38	0.92						250	20	1
GM CMa	4.52	3.10	2.22	1.39	0.76	0.54	0.30	0.22	403		21	94
V503 Mon	8.11	6.59	5.69	4.9:	0.60	0.40	0.16	0.16	357	355	20	11
RT Gem	6.51	5.21	4.62	4.21	0.76	0.74	0.58	0.72	350	350	10	9
06487+0551	9.14	6.58	4.62	2.24	1.34	1.20	1.02	0.74	536		10	12
CG Mon	5.33	3.96	3.30	2.75	0.82	0.74	0.60	0.70	424	419	10	9
CL Mon	4.78	3.06	1.88	0.59	1.28	1.02	0.74	0.52	511	497	10	10
06531-0216	6.95	4.89	3.35	1.61	1.32	1.18	0.98	0.64	595:		14*	13
NP Pup	2.49	1.38	1.03	0.64							20	3
06564+0342	10.26	7.59	5.43	2.84	1.50	1.32	1.16	1.02	584		10	12
W CMa	2.59	1.40	0.96	0.50							20	13
07080-0106	11.5	8.68	6.23	3.49		2.54	1.60	1.04	594		10	12
VX Gem	4.96	3.74	3.13	2.78	1.14	1.06	0.66	0.78	391	379	10	9
07097-1011	8.91	7.04	5.92	4.95	0.50	0.36	0.22	0.24	437		20	13
R Vol	5.08	3.14	1.71	0.08	1.46	1.26	0.98	0.80	452	454	11 [†]	88
HX CMa	7.92	5.46	3.62	1.42						725	10	1
07136-1512	8.12	6.50	5.57	4.74	0.36	0.28	0.16	0.10	486:		20	12
07161-0111	7.40	5.26	3.58	1.64							23	12
07217-1246	8.88	6.32	4.30	1.91	1.42	1.32	1.12	0.88	620:		10	12
07220-2324	9.51	6.80	4.77	2.46	1.58	1.24	1.06	0.88	560		10	13
07223-1553	7.98	6.23	5.23	4.38	0.56	0.44	0.24	0.18	457		20	13
07293-1832	8.80	6.99	6.02	5.17							20	12
07319-1940	7.91	6.36	5.64	4.99							20	6
[W71b]007-02	7.85	6.08	4.93	3.79	1.12	0.94	0.70	0.40	460:		13	15
07373-4021	5.39	3.52	2.23	0.77	1.40	1.20	0.90	0.78	459	471	13	15
[W71b]008-03	9.50	8.01	7.30								20	6
V471 Pup	7.08	5.78	5.13	4.63	1.04	0.98	0.76	0.92	390		10	16
[ABC89]Pup3	7.79	6.31	5.37	4.61	0.24	0.22	0.10		309		20	9
[ABC89]Pup17	9.42	7.86	7.12	6.54							20	6
07454-7112	8.03	5.08	2.82	0.07	2.08	1.98	1.72	1.46	511		10	11
[ABC89]Pup21	9.27	7.55	6.38	5.34							23	17
V831 Mon	6.53	4.99	3.89	2.76	1.38	1.04	0.74	0.58	331	319	10	13
07576-4054		9.29	6.62	3.39		1.98	1.80	1.40	519		10	16
07582-1933	10.70	7.74	5.39	2.69	1.84	1.82	1.62	1.42	541		10	14
V509 Pup	5.95	4.48	3.72	3.01							20	8
[ABC89]Pup38	10.65	8.79	7.43	6.06	1.26	1.08	0.88	1.00	431		10	15
FF Pup	6.64	5.38	4.69	4.00	1.10	1.16	0.94	1.06	431	436	10	8
[ABC89]Pup42	8.52	6.97	6.16	5.45	0.28	0.22	0.14	0.06	199		20	15
V518 Pup	6.96	4.90	3.52	2.07	1.06	0.94	0.76	0.80	228	448	13	13
08050-2838	10.40	7.28	5.08	2.57	2.10	1.80	1.48	1.26	555		13	11
RU Pup	3.65	2.52	2.04	1.48						425	20	2
FK Pup	3.55	2.16	1.46	0.78						502	20	2
08074-3615		13.13	9.09	4.50		2.14	1.74	1.46	832		10	13
[ABC89]Ppx19	9.98	7.77	6.11	4.23	1.78	1.30	0.88	0.46	474		13	16
[W71b]021-05	6.66	5.19	4.40	3.71							20:	4
[ABC89]Ppx22	6.59	5.10	4.34	3.62							20:	4
V346 Pup	8.67	5.92	3.75	1.16	1.78	1.60	1.38	1.14	568	571	10	51

Continued on Next Page...

Name	<i>J</i>	<i>H</i>	<i>K</i>	<i>L</i>	ΔJ	ΔH	ΔK	ΔL	P_K	P_{lit}	Var	no.
[W71b]026-01	8.27	6.51	5.58	4.72							20:	4
RY Hya	4.36	2.98	2.24	1.46	0.46	0.30	0.14	0.12	516	529	20	61
[ABC89]Ppx40	7.68	6.15	5.36	4.73	1.20	1.04	0.74	0.78	428	439	10	13
[W71b]029-02	9.48	7.28	5.63	3.86	1.06	0.92	0.72	0.52	470		10	19
[W71b]029-04	8.62	6.80	5.82	5.01							20:	4
08340-3357	11.29	8.14	5.61	2.56	2.32	1.56	1.46	1.16	590		10	18
R Pyx	4.55	3.28	2.53	1.81	>0.74	>0.46	>0.22	>0.34	369	365	13	11
UW Pyx	4.87	3.46	2.68	1.85						423	10	5
T Cnc	3.21	1.81	1.07	0.43						482	20	1
08535-4724		10.78	7.58	4.05		1.84	1.72	1.54	570:		13	14
08534-5055		11.96	8.50	4.55		2.56	1.92	1.60	703		10	15
IQ Hya	5.68	4.06	2.89	1.64	1.14	0.94	0.70	0.68	382	397	10	15
CQ Pyx		9.31	5.98	2.09		1.84	1.82	1.48	659		10	33
09164-5349	4.14	2.73	2.11	1.40							25 [†]	12
09176-5147	11.57	8.59	6.31	3.63	1.50	1.54	1.36	1.02	431:		13	16
[ABC89]Vel19	10.11	7.98	6.75	5.64							21	20
[W71b]046-02	9.03	7.27	6.38	5.78	1.00	0.76	0.40	0.34	265		10	15
[ABC89]Vel44	8.02	6.25	5.15	4.09	0.74	0.60	0.40	0.32	413		10	16
09433-6233	11.33	8.94	7.18	5.17	1.06	1.10	1.10	1.10	590:		13	12
CW Leo	7.34	4.04	1.19	-2.54	2.06	2.14	2.06	1.74	651	630	10	37
W Sex	5.11	3.95	3.49	3.06	0.32	0.26	0.16	0.12	195	134	20	17
09484-6242	7.63	6.27	5.56	4.89	0.06	0.10	0.08	0.06	244:		20	7
09513-5324	10.92	7.60	5.07	2.04	1.92	1.70	1.54	1.30	630		10	12
09529-5506	10.66	7.91	5.82	3.11	2.56	2.08	1.72	1.50	688:		10	8
09533-6021	12.78	9.54	7.03	4.04	1.96	1.90	1.72	1.38	714		10	12
09521-7508	8.11	5.36	3.22	0.70	1.98	1.96	1.74	1.28	539		10	9
09586-6150		12.02	9.19	5.90		1.78	1.68	1.38	506		10	11
10019-6156	7.87	6.55	5.99	5.49							20	7
10023-5946	6.94	5.53	4.90	4.20	0.32	0.26	0.18	0.12	571:		20	11
10026-5849	9.80	7.49	5.90	4.22	1.04	0.94	0.68	0.52	531		13	10
10052-5906		7.46	6.47	5.67	0.52	0.38	0.20	0.10	448		20	12
10098-5742		10.29	7.55	4.24		1.38	1.26	1.16	585		10	14
10109-5958	7.26	5.49	4.27	3.03	0.78	0.70	0.58	0.50	423:		13	11
RW LMi	6.18	3.43	1.32	-1.21	1.86	1.72	1.50	1.28	617	640	10	14
10130-5703	6.30	4.07	3.07	2.23							20	5
10136-5743	8.33	6.40	5.23	3.94							15: [†]	13
10145-6046	5.78	4.35	3.65	2.97							20	11
10149-5919	6.68	5.18	4.53	3.90							20	6
10151-6008	9.28	7.86	7.21	6.51							20	6
10175-5957	8.28	6.61	5.66	4.86							20	12
10199-5801	11.81	8.51	6.20	3.52	1.66	1.56	1.28	1.02	675		10	14
10220-5858	8.54	6.62	5.39	4.20	0.86	0.64	0.42	0.32	585:		10	11
CPD-58 2175	12.33	9.39	7.14	4.54	1.74	1.58	1.42	1.22	548		10	10
CZ Hya	4.73	3.32	2.39	1.38	1.42	1.30	0.96	0.92	444	442	10	12
[ABC89]Car5	9.76	8.28	7.53	6.83	0.20	0.20	0.14		168		20	12
[ABC89]Car11	8.50	6.99	6.17	5.41							20:	4
TV Vel	5.08	3.82	3.24	2.74	0.60	0.54	0.40	0.40	404	365	10	14
U Ant	1.24	0.01	-0.49	-1.11							20	25
[ABC89]Car28	8.95	7.29	6.36	5.47	0.56	0.42	0.24	0.20	495		20	16
[ABC89]Car32	7.67	5.85	4.84	3.90							20	15
FU Car	6.41	4.81	3.85	2.89	0.70	0.58	0.32	0.28	431:	365:	20	13
[ABC89]Car54	6.98	5.16	4.26	3.44	0.22	0.22			232:		20	6
[ABC89]Car59	7.22	5.56	4.62	3.78							20:	4
V Hya	1.78	0.29	-0.70	-1.86	>0.52	>0.42	>0.30	>0.28	532	531	22 [†]	75
[ABC89]Car73	10.69	8.10	6.34	4.41	1.88	1.32	1.06	0.84	483		10	14
[ABC89]Car81	9.12	7.28	6.28	5.46							20:	3
[ABC89]Car84	8.07	6.37	5.34	4.25	1.00	0.80	0.52	0.46	501		10	15
[ABC89]Car87	8.66	7.10	6.12	5.43	1.08	0.88	0.52	0.38	473		10	9

Continued on Next Page...

Name	<i>J</i>	<i>H</i>	<i>K</i>	<i>L</i>	ΔJ	ΔH	ΔK	ΔL	P_K	P_{lit}	Var	no.
[ABC89]Car93	8.64	6.64	5.54	4.56	0.72	1.06	0.86	0.44	416		10	12
[ABC89]Car105	7.32	5.47	4.24	2.91	0.90	0.70	0.46	0.34	497		11:*	15
11145–6534	10.00	6.93	4.49	1.69	1.72	1.72	1.58	1.46	623		10	12
[W65] c1	9.16	7.59	6.81								20	8
[W65] c2	8.03	6.70	6.26								24*	8
[W65] c13	8.68	6.92	5.85	4.91	0.96	0.74	0.44	0.34	395		10	14
[TI98]1130–1020	7.82	5.68	4.04	2.20	1.38	1.24	1.12	0.94	443		10	20
11318–7256	4.01	2.13	0.85	–0.66	1.38	1.14	0.90	0.68	526	535	10	9
[ABC89]Cen3	9.63	7.87	7.00								20:	5
[ABC89]Cen4	7.12	5.53	4.68	3.83	0.76	0.68	0.46	0.44	514		10	16
11463–6320	10.39	7.50	5.44	2.99	2.02	2.06	1.80	1.60	615		10	14
[ABC89]Cen32	8.95	6.67	5.05	3.28	1.14	1.04	0.84	0.70	652		10	14
[ABC89]Cen43	9.16	7.18	5.82	4.41	1.36	1.10	0.78	0.50	535		10	13
[ABC89]Cen60	8.66	6.84	5.71	4.56	1.02	0.86	0.60	0.68	414		10	13
[ABC89]Cen78	9.39	7.51	6.48	5.65	0.54	0.34	0.20		401		20	13
CF Cru	8.91	7.14	6.21		0.72	0.62	0.42		430		10	15
[ABC89]Cen97	10.3	7.90	6.57	5.27	2.12	1.32	0.80	0.46			23	14
12194–6007	9.59	7.00	4.96	2.57	1.66	1.54	1.26	0.94	627		10	12
SS Vir	2.93	1.56	0.75	0.01	0.92	0.68	0.36	0.20	359	364	20	55
12298–5754	9.28	6.65	4.40	1.70	1.56	1.66	1.54	1.24	580		10	10
CGCS3268	5.63	4.28	3.43	2.78						396	10	1
12394–4338	7.49	4.89	2.91	0.72	1.68	1.62	1.30	1.24	551		14*	12
12421–6217			8.47	4.50			2.40	2.02	806		10	8
RU Vir	4.86	3.09	1.80	0.29	1.40	1.24	0.98	0.90	444	433	10	46
V Cru	4.71	3.46	2.88	2.45	0.76	0.68	0.50	0.64	380	376	10	96
12540–6845	8.20	5.52	3.52	1.15	2.04	1.78	1.56	1.30	586		10	10
[ABC89]Cru17	10.16	8.39	7.45	6.15							20:	1
[ABC89]Cir1	7.91	5.95	4.85	3.56							25	11
13343–5807	9.75	7.04	4.98	2.57	1.86	1.88	1.62	1.42	556		10	13
13477–6532		9.67	6.62	2.78		1.46	1.68	1.36	690		10	13
13482–6716	8.47	5.79	3.78	1.49	1.66	1.66	1.44	1.18	500		10	12
13509–6348			5.12	2.72		1.70	1.46	1.36	678		10	16
[ABC89]Cir18	10.04	8.27	7.33	6.5							20	13
[ABC89]Cir26	9.13	6.71	5.12	3.36	1.74	1.36	0.96	0.74	495		10	15
[ABC89]Cir27	9.50	7.12	5.27	3.10	1.18	1.22	1.02	0.84	538		13*	12
[W71b]093–02	10.5	8.67	7.41								10:	4
14395–5656	9.15	7.21	6.01	4.73	0.86	0.66	0.44	0.28	488		10	11
14404–6320		11.46	8.32	4.39		2.08	2.18	1.70	643		10	9
14443–5708		12.77	8.93	4.94		2.98	2.16	1.80	723		10	8
15082–4808	10.00	7.00	4.36	0.86	1.76	1.68	1.64	1.48	632		10	13
15084–5702		10.85	7.33	3.37		2.38	2.36	1.94	948		10	10
II Lup	5.92	3.58	1.79	–0.33	1.04	0.92	0.82	0.88	576	580	11 [†]	28
15261–5702		8.45	5.96	3.07		2.34	2.02	1.40	716		10	15
15471–5644				7.78							10*	1
CGCS3660	6.82	5.67	5.38	5.19							20:	2
16079–4812		10.24	6.85	2.88		2.02	2.32	1.96	710		10	12
NP Her	5.79	4.36	3.50	2.79						448	10	1
16171–4759	9.58	6.89	4.89	2.70	1.26	1.28	1.06	0.86	560		13	14
V Oph	3.65	2.35	1.61	0.99	1.20	0.86	0.48	0.38	294	297	10	11
SU Sco	3.08	1.77	1.11	0.56						414:	20	5
CGCS3721	6.56	5.08	4.12	3.28						353	10	1
16406–1406		11.79	8.74	5.10							15:†	28
16538–4633	8.84	6.07	4.27	2.30	1.18	1.04	0.84	0.72	527		13	12
16545–4214	7.14	4.50	2.52	0.38	1.62	1.68	1.46	1.28	534		10	12
T Ara	4.53	3.27	2.77	2.27	0.20	0.12	0.10	0.08	327		20	13
V901 Sco	5.52	4.01	3.18	2.38	0.70	0.58	0.38	0.34	439:		20	10
17047–2848	9.45	7.09	5.36	3.28	1.88	1.74	1.52	1.38	531		10	12
V2548 Oph		8.48	5.61	1.98		2.08	2.06	1.80	747		10	40

Continued on Next Page...

Name	<i>J</i>	<i>H</i>	<i>K</i>	<i>L</i>	ΔJ	ΔH	ΔK	ΔL	P_K	P_{lit}	Var	no.
SZ Ara	6.16	5.00	4.45	4.06	0.94	0.68	0.44	0.42	222	220	10	8
V617 Sco	4.67	3.15	2.17	1.23	1.42	1.48	1.14	1.04		524	10	6
17105-3746	9.74	7.16	5.14	2.60	1.98	2.18	2.10	1.82	568		10	10
17130-3907	8.92	6.15	4.23	2.09	2.32	1.82	1.36	1.18	628		13	14
17209-3318E	12.63	9.04	6.24	3.18							10	4
17217-3916		9.30	6.42	3.14		1.90	1.94	1.60	630		10	11
17222-2328	9.67	6.66	4.60	2.30	1.88	1.74	1.58	1.48	603		13	9
V833 Her	9.58	6.66	4.19	1.00	2.36	2.80	2.72	2.10	540		13	13
V Pav	2.08	0.76	0.19	-0.39					437	225	20	69
17446-7809	7.22	4.69	2.72	0.55							10	4
17446-4048	8.15	5.54	3.60	1.47	1.34	1.24	1.10	1.18	545		13*	12
17463-4007	10.04	8.37	7.22	5.92	1.58	1.32	0.98	0.90	399		10	14
V348 Sco	7.09	6.11	5.66		0.26	0.30	0.26	0.12		274	20	6
17581-1744	8.26	5.77	4.03	2.12	1.70	1.40	1.08	0.94	628		10	8
18036-2344	10.71	7.37	4.93	2.17	2.66	2.78	2.22	1.96	664		13*	9
FX Ser	7.03	4.45	2.59	0.54	1.70	1.54	1.28	1.02	519		10	26
V1280 Sgr	5.33	3.58	2.39	1.02	1.10	1.02	0.78	0.70	532	523	13	57
18119-2244		8.39	5.60	2.65		2.24	1.82	1.56	611		10	12
18147-2215		9.92	6.50	2.91							10	5
V5104 Sgr	9.05	5.87	3.52	0.78	1.80	1.72	1.52	1.34	655		10	44
V2548 Sgr	4.47	2.96	2.11	1.22						159	23	11
18239-0655	10.31	7.23	4.64	1.69	1.58	1.48	1.44	1.24	635		10	9
18244-0815	11.4	8.58	5.97	3.27							10	6
V1076 Her		9.14	5.84	1.95		2.20	1.98	1.62	609		10	12
18248-0839	12.8	9.14	6.13	2.88			2.04	2.04	659:		10	7
18269-1257	13.1	8.98	5.85	2.53							10*	5
18320-0352		11.61	8.31	4.45							10	4
V627 Oph	7.90	5.97	4.66	3.17						452	10	3
18367-0452		10.47	7.11	3.17							10:	2
V1417 Aql	6.23	3.78	1.96	-0.08	1.30	1.10	0.92	0.72	617		13	25
18400-0704			8.28	4.64							10	3
V821 Her	5.98	3.68	1.85	-0.25	1.88	1.78	1.52	1.22	524	511	10	15
18424+0346	9.73	6.99	4.87	2.48							10	6
V874 Aql	8.71	7.61	7.22	6.79						145	10	3
V2045 Sgr	6.21	4.50	3.46	2.42						451	10	7
S Sct	2.43	1.13	0.57	0.05						148	20	16
18475+0926			5.91	2.36							10	3
AI Sct	6.12	4.50	3.48	2.63						408	10	5
V1418 Aql	8.29	5.44	3.14	0.47	2.02	1.74	1.42	1.08	562	577	10	20
19029+2017	8.17	5.68	3.87	1.86							10	5
19068+0544	8.01	5.41	3.75	2.07							10	7
V1420 Aql	5.94	3.68	2.08	0.06	1.68	1.44	1.22	1.18	694	676	12	18
V374 Aql	4.91	3.30	2.29	1.26						456	20	8
V1965 Cyg	7.64	5.00	2.95	0.55	2.52	2.08	1.68	1.26	577	625	13	11
19358+0917		11.91	8.36	4.46							10:	1
19455+0920	12.1	9.32	6.73	3.5							10	5
R Cap	5.31	3.94	3.05	2.09	1.42	1.18	0.86	0.96	349	345	10	15
RT Cap	2.48	1.15	0.54	-0.06	0.30	0.24	0.14	0.10	359	393	20	23
BD Vul	5.84	4.30	3.37	2.63						430	10	4
V442 Vul	9.78	6.84	4.22	1.14	2.14	2.28	2.02	1.56	661		10	12
RV Aqr	4.68	2.75	1.39	-0.13	1.58	1.32	1.04	0.94	433	454	10	7
Y Pav	1.89	0.69	0.26	-0.08						233	20	2
[TI98]2259+1249	6.97	5.78	5.24	4.90	0.78	0.74	0.54	0.68	306	294	10	36
LL Peg			10.50	4.27						696	10	7
RU Aqr	3.10	2.08	1.78	1.51						69	20	1
IZ Peg		10.26	7.09	3.04		1.98	1.94	1.56	486	486	10	103
[TI98]2223+2548	7.19	5.56	4.35	3.06	1.40	1.18	0.90	0.80	343		10	16

Continued on Next Page...

Name	<i>J</i>	<i>H</i>	<i>K</i>	<i>L</i>	ΔJ	ΔH	ΔK	ΔL	P_K	P_{lit}	Var	no.
CS stars, peculiar and uncertain C stars												
R Ori	5.82	4.70	4.15	3.76	0.92	1.00	0.78	0.96	381	377		14
R CMi	4.03	2.97	2.48	2.22	0.88	0.82	0.86	0.74	335	338		12
08276–5125			11.69	6.63								1
08439–2734	6.56	4.85	3.79	2.40	1.66	1.52	1.28	1.26	475			14
UX Pyx	3.93	2.91	2.59	2.26						423		1
MU Vel			9.49	5.30		1.54	1.56	1.48	597			33
10226–5229	8.89	6.25	4.56	2.60	2.98	2.32	1.86	1.50	756			10
[ABC89]Car10	7.00	5.59	4.99	4.37	1.14	1.00	0.88	0.88	397			15
TU Car	7.16	6.07	5.52	4.92	0.78	0.86	0.74	0.58	254	258		10
V354 Cen	9.22	8.33	8.04	7.6	0.38	0.32	0.18		150	150		11
[ABC89]Cen50	9.73	7.54	6.01	4.34	0.92	0.82	0.70	0.60	512			12
BH Cru	3.21	2.03	1.56	1.23	0.62	0.66	0.58	0.64	491	421		46
BH Cru	3.15	1.98	1.40	1.01	0.72	0.70	0.50	0.64	524	421		36
TT Cen	4.35	2.99	2.43	1.91	>0.72	>0.76	>0.68	>0.80	448	462		89
RV Cen	3.33	2.08	1.47	1.00	0.68	0.56	0.36	0.46	447	446		87
16316–5026	4.28	2.56	1.82	1.00	1.48	0.96	0.84	0.74	565			13
VX Aql	4.90	3.59	3.06	2.41						604		2
18595–3947	3.30	1.52	0.51	–0.69	2.02	1.50	1.10	0.98	449			22
V1293 Aql	2.10	1.11	0.83	0.59								5

†These stars are discussed in the section 11 on long term trends.

*These are stars for which the second parameter of the variable type depends on the combination of our observations and photometry from other sources. **V718 Tau** Epchtein et al. (1990) and 2MASS data obtained before and after SAAO observations, at phases which are similar to our faintest measurements (i.e. not in the gap) suggest that it has been much fainter ($K=3.94$, 3.88 respectively, $\Delta K \sim 0.7$) and redder, than the faintest SAAO measurements. **05418–3224** An observation by Epchtein et al. (1990) predating ours is 3 and 5 mag brighter at K and J respectively. 2MASS photometry contemporaneous with ours and Fouqué et al. (1992) measurements predating ours are within the range shown in our light curve. We therefore class this star as showing obscuration events, but note that the evidence is very limited. **V617 Mon** Although Noguchi et al. (1981) present measures distinctly different from ours, a comparison with 2MASS suggests they actually observed BD+08°1312, an M star about one arcmin away from V617 Mon. **06531–0216** Note that the 2MASS ($K = 4.45$) and Epchtein et al. (1990) ($K = 2.89$) observations do not agree with the phasing of the SAAO data. The period must therefore be regarded as uncertain. **[ABC89]Car105** The Aaronson et al. (1989) observation ($K = 5.41$), which predates the SAAO photometry, is much fainter than our minimum ($K = 4.48$). This may indicate an obscuration event. **[W65] c2** While the 2MASS, the 1985 Aaronson et al. (1989) and the SAAO observations differ by less than 0.1 mag at K , the 1988 Aaronson et al. photometry is considerably fainter ($J = 9.14$, $K = 7.21$). **12394–4338** The Fouqué et al. (1992) observation ($J = 8.55$, $K = 4.48$) is significantly fainter at K , but not at J , than the SAAO minimum ($J = 8.60$, $K = 3.74$), while the 2MASS and Epchtein et al. (1990) observations are comparable to those listed here. **[ABC89]Cir27** The Aaronson et al. (1989) measurement ($K = 3.87$) is significantly brighter than the SAAO maximum ($K = 4.57$) and may indicate that the source was obscured during the SAAO observations. **15471–5644** Too crowded for measurement at JHK , but 2MASS has $K = 14.8$ and Groenewegen et al. (1993) have $K = 11.4$, $L = 4.6$, so it is certainly a large amplitude variable. **17446–4048** The Fouqué et al. (1992) measurement ($K = 4.81$) is significantly fainter than the SAAO minimum ($K = 4.21$) and may indicate the star was being obscured at the time the observation was made. 2MASS is also faint ($K = 4.65$). **18036–2344** The Guglielmo et al. (1993) measurement ($K = 6.53$) is significantly fainter than the SAAO minimum ($K = 5.81$) and may indicate that the star was in an obscuration phase. **18269–1257** 2MASS has $K = 8.02$ on JD 2450937, so all our observations are near maximum and $P \sim 700$ days.

Some of the photometry discussed in the present paper has already been published by Whitelock et al. (1994, 1995, 1997, 2000), Olivier et al. (2001), Feast et al. (1985, 2003), Groenewegen et al. (1998) or by Lloyd Evans (1997). All of these data are included in the electronic table for ease of reference. A small number of measurements were made at SAAO as part of other programmes by T. Lloyd Evans and/or by S. Bagnulo and I. Short. These are used in the means quoted and in the diagrams, but the basic data will be published elsewhere. Individual observations of some objects also appeared in other papers without dates (e.g. Gaylard & Whitelock 1988; Gaylard et al. 1989); these measurements are included in the present tabulation.

3.1 IRAS and MSX data

Because energy distributions of C stars typically peak between 3 and 10 μm , a measure of the energy output beyond the *L* band is important for estimating their bolometric flux. Following earlier work (e.g. Whitelock et al. 2000, 2003) we use the IRAS 12 and 25 fluxes and, where possible, supplement these with data from the MSX survey (Egan et al. 2003) using the *A*- (8.28 μm), *C*- (12.13 μm) and *D*- (14.65 μm) bands.

IRAS photometry was taken preferentially from the IRAS Faint Source Catalogue (FSC Moshir et al. 1989) or from the PSC (IRAS Science Team 1989). The IRAS fluxes for CW Leo were taken from the PSC rather than the FSC as these were more consistent with comparable values from the literature (Gezari, Pitts & Schmitz 1997). The IRAS photometry was colour corrected using the prescription from the IRAS explanatory supplement for the purpose of calculating bolometric magnitudes only. For the discussion of colours etc. the raw magnitudes were used.

There are 18 stars which have no IRAS fluxes, but 13 of these have been measured in the MSX *A*-band. The remaining 5 sources all have $K - L < 1.0$ and the long wavelength fluxes will not make a significant contribution to their bolometric magnitude (in fact one of them, V354 Cen, is probably not a C star and only two, V874 Aql and [ABC]Car93, are classed as C Miras).

The MSX data were extracted from the complete MSX6C catalogue in the Galactic Plane ($|b| \leq 6^\circ$) and the high latitude, $|b| > 6^\circ$, subsections only. A few of our sources have detections in the low reliability sources ([ABC89]Car5) and singleton source (extracted from a single scan but with good fluxes: Y Tau, CL Mon, 07080–0106, 07220–2324, FF Pup, 08340–3357, MU Vel, 09533–6021, 10145–6046, TV Vel, 11145–6534) sections of the catalogue, but a close examination suggested these were unreliable, e.g. some singleton sources showed unphysical colours.

The very bright sources appear to be saturated in the MSX-*A* band, which is more sensitive than any of the others, as can be seen in the plot of *A* – *C* against *C* (Fig. 1). The four very bright stars are II Lup, V1417 Aql, V1418 Aql and V1965 Cyg. Their MSX-*A* magnitudes are inconsistent with other MSX and IRAS magnitudes, although this is not clear from the flags provided with the catalogue. It appears that among this type of object anything brighter than 270 Jy at *C* will be saturated at *A*.

Note also from Fig. 1, the difference in the *A*–*C* colours of stars, particularly Miras, that are brighter and fainter

Table 3. Individual *JHKL* Observations (Full table available electronically).

JD (day)	<i>J</i>	<i>H</i>	<i>K</i>	<i>L</i>	Tel.
(mag)					
R Scl					
2443123.5	1.75	0.60	–0.03	–0.62	
2443405.5	2.04	0.76	0.01	–0.54	
2444187.2	1.87	0.61	–0.04	–0.67	
2446265.8	2.17	0.74	–0.05	–0.79	
2446300.5	2.44	0.95	0.09	–0.74	
2446303.5	2.53	1.03	0.13	–0.61	
2446334.5	2.55	1.07	0.15	–0.64	
2446356.5	2.55	1.06	0.13	–0.65	
2446373.5	2.46	0.98	0.10	–0.70	
2446391.2	2.43	0.96	0.10	–0.69	
2446640.5	2.02	0.62	–0.14	–0.83	
2446655.5	2.15	0.71	–0.09	–0.80	
2446662.5	2.18	0.75	–0.07	–0.84	
2446690.5	2.40	0.91	0.02	–0.76	
2446695.5	2.44	0.97	0.08	–0.68	
2446712.5	2.53	1.02	0.11	–0.67	
2446741.5	2.54	1.04	0.13	–0.63	
2446749.5	2.50	1.00	0.11	–0.62	
2446754.2	2.45	0.98	0.09	–0.67	
2446775.2	2.31	0.88	0.05	–0.62	
2446782.2	2.26	0.85	0.03	–0.64	
2446805.2	2.14	0.77	0.02	–0.56	
2446984.8	1.61	0.33	–0.28	–0.90	
2447014.5	1.80	0.44	–0.26	–0.94	
2447056.5	2.15	0.69	–0.13	–0.88	
2447073.5	2.28	0.79	–0.09	–0.84	
2447113.5	2.32	0.86	–0.03	–0.74	
2447144.2	2.19	0.75	–0.07	–0.79	
2447176.2	2.07	0.67	–0.07	–0.65	
2447191.2	2.03	0.67	–0.08	–0.66	
2447364.8	1.62	0.32	–0.35	–0.98	
2447379.5	1.70	0.36	–0.31	–1.03	
2447394.5	1.73	0.41	–0.32	–1.01	
2447427.5	2.02	0.61	–0.19	–0.94	
2447447.5	2.16	0.73	–0.12	–0.89	
2447497.2	2.36	0.92	0.01	–0.69	
2447512.2	2.30	0.88	0.01	–0.73	
2447534.2	2.19	0.80	–0.04	–0.72	
2447732.8	1.56	0.27	–0.35	–0.93	
2447745.5	1.55	0.25	–0.38	–1.03	
2447761.5	1.57	0.26	–0.39	–1.01	
2447779.5	1.74	0.38	–0.31	–1.01	
2447805.5	2.03	0.61	–0.18	–0.88	
2447816.5	2.14	0.74	–0.09	–0.88	
2447821.5	2.21	0.78	–0.06	–0.84	
2447841.5	2.42	0.96	0.05	–0.77	
2447873.5	2.54	1.11	0.16	–0.61	
2448073.8	1.98	0.65	–0.05	–0.68	
2448077.8	1.96	0.64	–0.05	–0.73	
2448109.8	1.91	0.55	–0.14	–0.74	
2448141.8	2.00	0.61	–0.12	–0.77	
2448172.5	2.13	0.70	–0.08	–0.78	
2448211.2	2.43	0.96	0.08	–0.67	
2448224.5	2.50	1.03	0.11	–0.69	
2448252.2	2.53	1.06	0.14	–0.61	
2448280.2	2.41	0.97	0.10	–0.58	
2448492.5	1.76	0.46	–0.19	–0.87	
2448519.5	1.92	0.55	–0.16	–0.85	
2448873.5	1.82	0.47	–0.22	–0.88	
2448900.5	2.03	0.62	–0.15	–0.87	

continued in the next column...

Table 3. continued...

JD (day)	<i>J</i>	<i>H</i> (mag)	<i>K</i>	<i>L</i>	Tel.
2448933.5	2.29	0.81	-0.04	-0.82	
2448960.2	2.41	0.92	0.04	-0.75	
2448990.2	2.42	0.94	0.04	-0.73	
2449000.2	2.41	0.94	0.04	-0.70	
2449022.2	2.26	0.86	0.02	-0.65	
2449146.8	1.83	0.56	-0.08	-0.65	
2449204.8	1.61	0.35	-0.27	-0.84	
2449212.8	1.62	0.35	-0.28	-0.86	
2449271.5	1.63	0.35	-0.28	-0.87	
2449223.5	1.65	0.35	-0.28	-0.88	
2449236.5	1.67	0.37	-0.29	-0.85	
2449263.5	1.85	0.48	-0.24	-0.92	
2449282.5	2.01	0.60	-0.18	-0.88	
2449289.5	2.09	0.65	-0.15	-0.92	
2449296.2	2.14	0.69	-0.14	-0.86	
2449346.2	2.37	0.90	0.01	-0.76	
2449497.8	1.73	0.47	-0.16	-0.69	
2449518.8	1.68	0.44	-0.17	-0.70	
2449581.5	1.46	0.24	-0.34	-0.90	
2449614.5	1.64	0.34	-0.29	-0.95	
2449637.5	1.88	0.50	-0.22	-0.89	
2449642.5	1.93	0.56	-0.19	-0.96	
2449668.5	2.33	0.89	0.03	-0.78	
2449672.5	2.37	0.92	0.04	-0.72	
2449709.2	2.57	1.11	0.16	-0.62	
2449728.2	2.53	1.09	0.16	-0.64	
2449772.2	2.25	0.85	0.03	-0.65	
2449941.8	1.71	0.43	-0.16	-0.70	
2449975.5	1.84	0.51	-0.18	-0.83	
2449986.5	1.95	0.58	-0.12	-0.73	
2450019.5	2.25	0.83	0.00	-0.72	
2450029.2	2.34	0.90	0.04	-0.66	
2450052.5	2.52	1.04	0.13	-0.61	
2450057.2	2.54	1.08	0.15	-0.64	
2450062.2	2.55	1.09	0.15	-0.65	
2450082.5	2.59	1.13	0.18	-0.62	
2450109.2	2.50	1.03	0.14	-0.59	
2450144.2	2.24	0.84	0.04	-0.55	
2450260.8	1.81	0.55	-0.07	-0.60	
2450274.5	1.69	0.45	-0.14	-0.66	
2450299.5	1.48	0.28	-0.27	-0.82	
2450317.5	1.43	0.24	-0.30	-0.84	
2450362.5	1.73	0.42	-0.25	-0.88	
2450398.2	2.19	0.76	-0.07	-0.80	
2450414.5	2.37	0.91	0.03	-0.71	
2450420.5	2.43	0.96	0.06	-0.69	
2450437.2	2.55	1.05	0.14	-0.70	
2450469.2	2.52	1.04	0.10	-0.66	
2450471.2	2.50	1.01	0.08	-0.64	
2450503.2	2.25	0.83	-0.02	-0.69	
2450681.5	1.61	0.35	-0.26	-0.77	
2450712.5	1.67	0.38	-0.27	-0.83	
2450721.5	1.73	0.42	-0.26	-0.82	
2450753.5	2.03	0.63	-0.13	-0.80	
2450792.2	2.33	0.87	0.00	-0.76	
2450830.2	2.40	0.92	0.02	-0.71	
2451025.2	1.64	0.40	-0.20	-0.76	
2451052.2	1.56	0.34	-0.26	-0.79	
2451115.5	1.87	0.50	-0.20	-0.86	
2451154.2	2.26	0.82	-0.01	-0.82	
2451186.2	2.49	1.01	0.10	-0.69	
2451417.5	1.61	0.38	-0.22	-0.75	
2451481.5	1.64	0.31	-0.33	-0.95	

*continued in the next column...***Table 3.** continued...

JD (day)	<i>J</i>	<i>H</i> (mag)	<i>K</i>	<i>L</i>	Tel.
2451502.5	1.75	0.38	-0.31	-0.94	
2451575.2	2.33	0.86	-0.04	-0.78	
2451600.2	2.39	0.91	0.01	-0.71	
2451738.8	1.80	0.54	-0.09	-0.70	
2451743.8	1.76	0.51	-0.11	-0.68	
2451782.5	1.55	0.33	-0.24	-0.83	
2451785.5	1.58	0.33	-0.25	-0.87	
2451859.5	1.75	0.41	-0.27	-0.98	
2451869.5	1.81	0.46	-0.25	-0.93	
2451881.2	1.89	0.52	-0.20	-0.94	
2451809.5	1.57	0.29	-0.31	-0.90	
2451831.5	1.62	0.32	-0.31	-0.91	
2451929.2	2.26	0.81	-0.04	-0.79	
2452182.5	1.57	0.30	-0.28	-0.87	
2452208.5	1.55	0.26	-0.35	-1.00	
2452226.2	1.63	0.32	-0.34	-0.98	
2452241.2	1.72	0.38	-0.30	-0.95	
2452257.2	1.88	0.50	-0.25	-0.94	
2452285.2	2.14	0.71	-0.09	-0.86	
2452321.2	2.45	0.98	0.06	-0.68	
2452529.5	1.76	0.49	-0.15	-0.78	
2452572.5	1.69	0.38	-0.27	-0.88	
2452602.2	1.75	0.43	-0.26	-0.89	
2452691.2	2.32	0.87	-0.01	-0.75	
2452888.5	1.64	0.39	-0.23	-0.81	
2452932.5	1.61	0.37	-0.28	-0.89	
2452960.5	1.69	0.38	-0.28	-0.96	

Some of these observation of R Scl were published by Lloyd Evans (1997) and by Whitelock et al. (1995, 1997).

than $C \sim 1$ mag. This occurs because the bright Miras are intrinsically different from the faint ones - the stars with large colour indexes, i.e. the “red” stars, are all relatively bright. There are various selection effects contributing to this, but critically we would have been unable to perform *JHK* photometry of faint red stars. A similar dichotomy is seen in the IRAS data, in that most of the Miras with $[12] > 0$ have $[12 - 25] < 0.5$ and those with $[12] < 0$ have $[12 - 25] > 0.5$. There are, however, some notable faint non-Miras with $[12 - 25] > 1$: EV Eri (see Section 11), 10151-6008, [ABC89]Cru17 and [ABC89]Cir1.

Figs. 2 & 3 illustrate the types of two-colour diagram which are frequently used to distinguish between O- and C-rich stars (e.g. Ortiz et al. 2005) using IRAS and MSX data respectively. The solid line on both figures is the blackbody locus, while the dashed line provides a rough division between C- and O-rich stars, which in the case of the MSX figure has been copied directly from Ortiz et al. The division is far from being a precise one and stars close to the line must be regarded as having uncertain chemical type unless spectroscopic information is available. Nevertheless, most of the programme stars fall in the region you would have expected given their C-rich nature. A similar separation can be achieved using slightly different combinations of colours, as was discussed, e.g., by Guglielmo et al. (1993).

In the MSX diagram the four peculiar non-Miras lying above the upper line are: 09164-5349 (see Section 11), [ABC89]Cir1, V2548 Sgr and [ABC89]Cru17, the latter being the only point well away from the line (NB the differ-

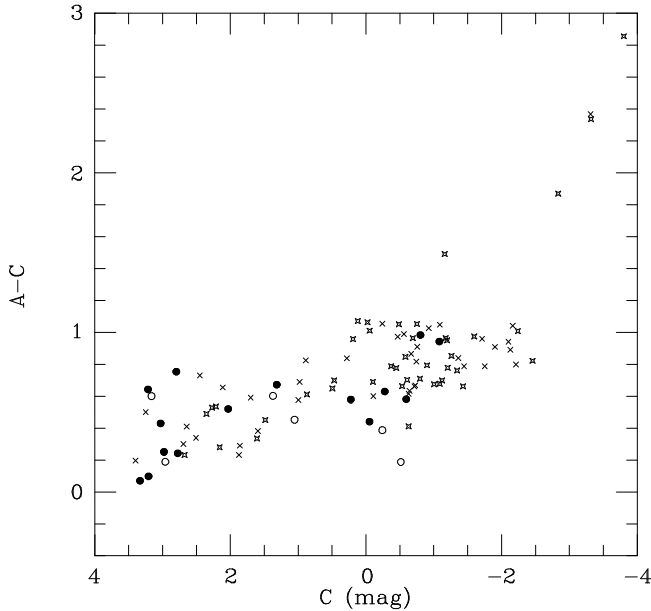


Figure 1. The MSX $A - C$ colour as a function of the MSX- C magnitude. Symbols: crosses: well observed Miras without obvious peculiarities; open crosses: other Miras; open circles: well observed small amplitude variables without obvious peculiarities; close circles: other non-Miras. The four sources with large $A - C$ colours are saturated in the A band. Note the difference between the typical $A - C$ colour for the stars brighter and fainter than $C \sim 1$, particularly the Miras.

ences between Miras and non-Miras and between ‘peculiar’ and ‘normal’ relate to the variability characteristics and are described in Section 4.2). The normal non-Mira above the line is [ABC89]Pup3. The stars in a comparable position on the IRAS diagram are these same peculiar non-Miras plus EV Eri and 10151-6008, while the normal non-Miras are R Scl (which has a detached dust shell, Bujarrabal & Cernicharo 1994) and T Ara (which is super lithium rich, Feast 1954).

4 PULSATION CHARACTERISTICS

4.1 Pulsation Periods

Periods (P_K) were determined from a Fourier transform of the K light curve for all of the stars with SAO near-infrared observations on 8 or more dates; these are listed in Table 2. Where a pulsation period has been published elsewhere it is listed in column 11 (P_{lit}) of Table 2. These are taken from the following sources, in order of preference: GCVS, Le Bertre (1992), Jones et al. (1990), Hipparcos (ESA 1997) or Pojmański (2002). Figure 4 shows our period plotted against the value from the literature. The agreement is generally better than 5 percent and a brief discussion of the exceptional cases follows:

V477 Mon The original period is from Maffei (1966) who indicated it as “M? P=820:: days”. The near-infrared observations are not consistent with this value and we use the newly determined 619 days which provides a very good fit to these data.

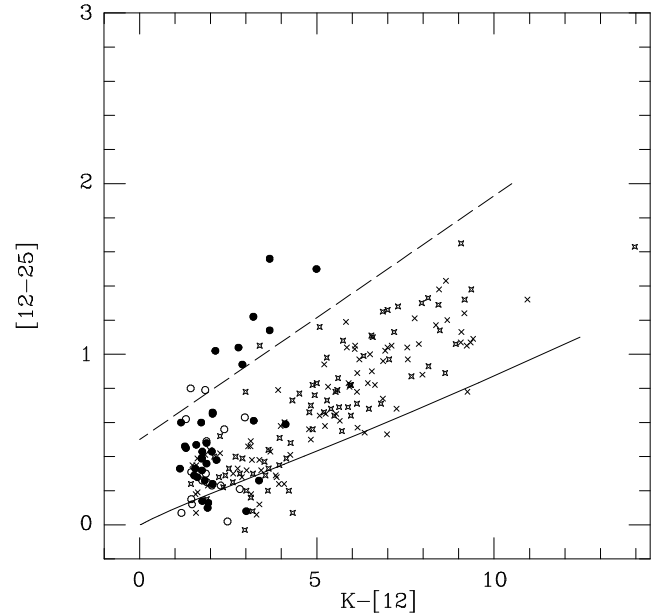


Figure 2. Combined IRAS near-infrared two-colour diagram; symbols as in Fig. 1. The solid line is the blackbody locus while the dashed line roughly separates C- from O-rich stars. Note that sources selected according to the IRAS selection criterion described in Section 2 will only find sources with $[12 - 25] > 0.565$. Symbols are the same as in Fig. 1.

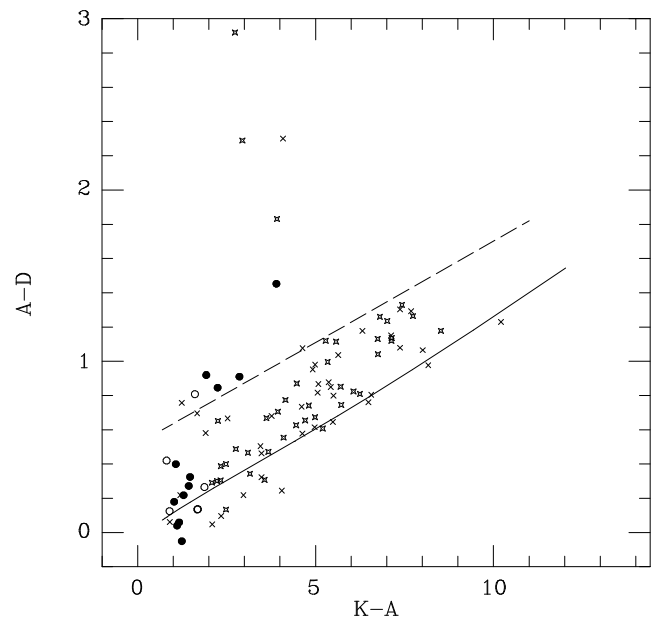


Figure 3. Combined MSX near-infrared two-colour diagram; symbols and lines as in Fig. 2.

V1965 Cyg The original period is from Jones et al. (1990) (who incorrectly associates AFGL 2417 with V1129 Cyg) and there is evidence for rather erratic behavior in both their and our light curves. Analyzing the two data sets together (using only the 6 observations actually listed in their paper) suggests a period of 617 days.

BH Cru This is known to have a lengthening period (Bateson et al. 1988; Walker et al. 1995; Zijlstra et al. 2004)

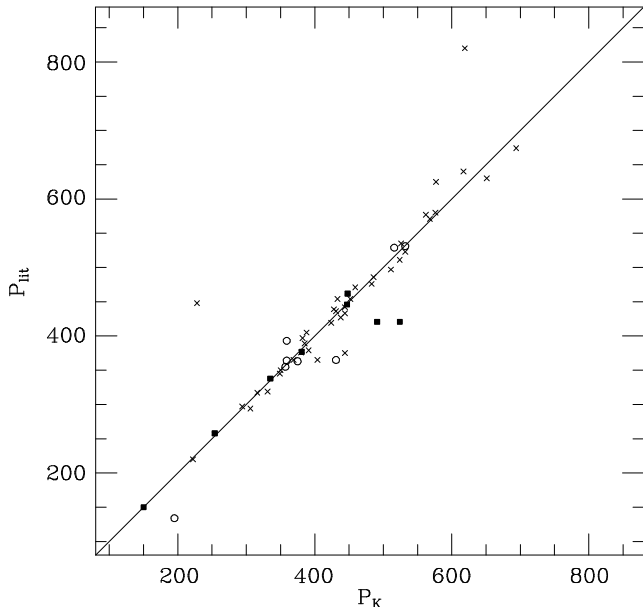


Figure 4. Periods, P_K , derived from data discussed here plotted against those from the literature, P_{lit} ; Symbols: crosses are Mira C-stars (outstanding points represent V477 Mon and V518 Pup), open circles are non-Mira C stars; solid squares are various peculiar sources including non-C stars, SC stars and C-stars with silicate shells (the two outstanding points represent BH Cru, which has a variable period, at different times).

and our data, which were obtained in two batches with a gap in the middle, suggests a change from 491 to 524 days, between 1984/9 and 1997/2004.

V617 Mon The GCVS period is 375: days with which the near-infrared observations are not consistent. We use the newly determined 444 days which provides a very good fit to our data.

FU Car The GCVS variability type and period of M: and $P=365$: days respectively, come from Luyten (1927) who records FU Car’s variability along with that of another star and notes “The available plates are insufficient for a determination of the light curves, but the possibility is indicated that both variables have a period of nearly one year, and a range of at least two magnitudes”. This is consistent with our determination of 431 days and our assertion that it is not a Mira.

TV Vel GCVS records this as variability type M with $P=365$ days and no indication of any uncertainty. There is no clear source for the period. We also classify TV Vel as a Mira, but it is certainly a border-line case. Our data are inconsistent with the 365 day period.

W Sex The difference between the GCVS period of 134 days and the Hipparcos period of 200 days was noted by Whitelock et al. (2000). Our newly determined period of 195 days is consistent with the Hipparcos value. It is not a Mira.

RT Cap This is not a Mira and the GCVS period of 393 days is inconsistent with the 359 days derived here.

V518 Pup The 448 day period comes from the ASAS database of Pojmański (2002) who also classifies it as a Mira. The 228 day period derived from the IR data is inconsistent with the ASAS data. While 228 days is the best fit to the

infrared photometry, 448 days is also a possible solution. In this case 448 days would be preferred and is in fact the value we adopt, but the Mira classification must be regarded as uncertain.

Figs. A-1 and A-2, in the appendix, illustrate for Miras and other variables, respectively, the K light curves plotted as a function of phase for the stars with sufficient data to determine a period.

From this it can be seen that the accuracy of the derived periods and amplitudes varies considerably from one star to the next, depending on the number of observations, their distribution in time and the stability of the light curve over the sampling interval. Most of the illustrations show the K magnitude phased at the period determined from the K data. Where satisfactory periods could not be determined from our data they are shown phased at the GCVS period. For 10220–5858 a period of 585: days is given, but 290: is also possible. Although we use the 585 day period in the following discussion the blue colours and low amplitude would fit better with the shorter period.

4.2 Variability Class

In view of the fact that we wish to use the Mira Period-Luminosity (PL) relation to estimate the distance to the C-stars it is vital that we decide if particular stars can be classed as Miras or not. According to the classical GCVS definition Miras have characteristic late-type emission spectra (Ce in the cases we are discussing) and V light amplitudes greater than 2.5 mag. Their periodicity is well pronounced, and periods lie in the range from 80 to 1000 days. For many of the stars of interest very little is known about the V magnitude and we must make the best estimate we can from other sources of information. Unfortunately the distinction between Miras and other types of long period variable is not as clearcut for C-rich stars as it is for O-rich ones, where the JHK_L colours of Miras and non-Miras are distinctly different (e.g. Whitelock et al. 1995).

Where there are sufficient observations we determine if a star is a Mira or not on the basis of the SAAO infrared photometry; if it is clearly periodic and has a peak-to-peak K amplitude over 0.4 mag we call it a Mira and assign it to class 1n. If the variations are not periodic or are less than 0.4 mag at K we assign it to class 2n, and call it a non-Mira. If there are insufficient data to do this we use the GCVS or ASAS classification if there is one. Otherwise, if our K magnitudes differ from published values (Aaronson, 2MASS ...) by 0.4 mag or more we assign it to class 1n else to class 2n. Stars classified in this last way are labeled with a colon after the classification in Table 2 as they are clearly less certain than the others. There are 74 class 2n and 165 class 1n in the table.

The assignment of the second digit, or sub-class, of the variability classification is described in Table 4. The sub-class to which a variable is assigned obviously depends strongly on how many observations we have, e.g. many objects of type 13 would probably be classed as type 11 given more data. There is actually only one star, V1420 Aql, catalogued as type 12, which is illustrated in the last panel of Fig. A-1, although there are several marginal cases, e.g. [ABC89]Cir27, as can be seen from the illustrated light curves. Even with V1420 Aql there is some uncertainty in

Table 4. Second parameter, n , of the variability type 1n or 2n.

n	description of light curve
0	sinusoidal and reasonably repeatable
1	evidence of obscuration events or a long term trend
2	for pronounced second peak in light curve (Miras only)
3	for erratic behavior, includes large amplitude non-Miras
4	inconsistent with other published photometry
5	star with peculiarities described in text

its period and if it is plotted at the other period given in Table 2 (676 days from Le Bertre 1992) then the second peak is less pronounced.

Our classification agrees reasonably well with the GCVS for most of the 102 stars in common and we briefly discuss the 10 differences here. We classify the following stars as Miras whereas the GCVS provided the classification given in parenthesis after the name: V471 Pup (SR:), V518 Pup (SR: also Mira in ASAS), UW Pyx (Lb: also Mira in ASAS), RW LMi (SRa), CF Cru (Lb), FX Ser (Lb:). The ASAS classification, based on optical data, is relevant as they have many more observations than we do and can do a better job with classifying visually bright variables. However, we agree with the GCVS classification of V374 Aql (SR) rather than the M: assigned by ASAS. The following were classed as Miras in the GCVS: FU Car, V354 Cen, V348 Sco and V503 Mon, but are classed as non-Miras here, because their K amplitudes are much less than expected from Miras.

The Mira nature of 10220–5858 is uncertain, it has a low amplitude and small $K - [12]$ for its period and limited data suggest an erratic light curve.

A number of authors have noted that the IRAS colours of [ABC89]Cir1 are those expected for a silicate shell (e.g. Chen et al. 1993 and references therein) and it has been investigated on this basis. We note that it has a slightly larger $K - L$ than normal non-Miras.

Of the 57 C stars in the Aaronson sample, 26 are Miras, and periods in the range 265 to 652 days have been determined for 24 of them, while the other 31 are erratic or low amplitude variables.

Of the 93 C-stars in the IRAS sample, 86 are Miras and periods ranging from 431 to 948 days were determined for 69 of them, while the other 7 are low amplitude or erratic variables. Of the 26 C-stars in the faint IRAS sample 12 are Miras, and periods in the range 495 to 714 days were determined for 10 of them, while the other 14 are erratic or low amplitude variables.

4.3 Mean Magnitudes and Amplitudes

Table 2 gives the Fourier-mean magnitudes and amplitudes for all of the stars discussed here. These were derived by fitting first order sine curves to the light curves, and the peak-to-peak amplitudes of those curves are also tabulated. The number of points used in the fit is listed in the last column. This may be less than the full number of observations available, as it is for stars showing obscuration events where we have excluded cycles showing heavy obscuration (see section 11). This is somewhat subjective and the results dependent on how well any particular light curve is covered.

The pulsation amplitude generally decreases with increasing wavelength, although there are a few examples of $\Delta J < \Delta H$. Where the source is faint at J a low amplitude may indicate contamination of the J flux by another source in the aperture; there are, however, examples, e.g. CW Leo, where the measured amplitudes are definitely a true reflection of the C star variations. Fig. 5 shows the dependence of pulsation amplitude on colour. Although there is a great deal of scatter, the amplitude and colour are clearly correlated. While there will be several effects contributing to this dependence, the primary one will be the amplitude's direct or indirect dependence on temperature fluctuations of the star. We also anticipate a correlation between the stellar pulsation amplitude, as measured by ΔK , and the mass-loss rate, as measured by $K - [12]$ which is proportional to the optical depth of the shell (see section 6 and Whitelock, Pottasch & Feast (1987). It is not possible to separate the effects of temperature fluctuations and pulsation amplitude changes with the available information.

The peaks of the energy distributions for these stars is at wavelengths over $2.5\mu\text{m}$ (the combined effect of low temperature and thick circumstellar dust shells), therefore at J and H and usually also at K and L , we are sampling the Wien part of the energy distribution which is extremely sensitive to temperature fluctuations. The cooler the star the larger the flux changes at $JHKL$ that will be caused by small changes of the stellar temperature. Molecular opacity fluctuations in the $JHKL$ bands, also in response to temperature changes of the star, will serve to magnify the amplitude dependence on stellar temperature. Thus to a first approximation we might expect the $JHKL$ amplitudes to tell us more about the temperature of the C star, and changes in its temperature around the pulsation cycle, than about the bolometric amplitude of the pulsations themselves. The colours that we discuss here, including $K - [12]$, are much more strongly influenced by reddening of the circumstellar shell than they are by the temperature of the underlying star (see Section 6). Nevertheless, the cooler stars will tend to have the thicker dust shells, so we still understand the correlation in Fig. 5 to be very considerably a consequence of fluctuations in the stellar temperature, but with a good deal of scatter as the thickness of the shell is not a simple function of the temperature of the star.

5 MIRA PERIOD-LUMINOSITY RELATION

The existence of a PL relationship for Mira variables was discussed in detail by Feast et al. (1989) for O- and C-rich Miras in the LMC. Subsequently Whitelock et al. (2003) discussed the PL relation for longer-period, thick-shelled Miras also in the LMC, including photometry from IRAS and ISO. The studies by Feast et al. and by Whitelock et al. encompassed stars with multiple near-IR observations and therefore well defined mean magnitudes. Groenewegen & Whitelock (1996) used data for spectroscopically confirmed C stars only, but included those with single observations to provide a larger sample of LMC stars. All of these papers found rather similar bolometric PL relations for the C stars.

Here we combine the data from Feast et al. (1989) and Whitelock et al. (2003) to derive a PL relation for the C stars that covers the period range of interest for the Galac-

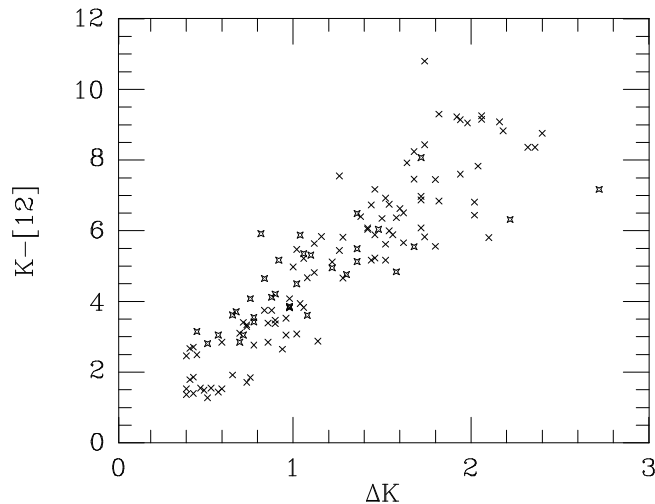


Figure 5. For the Miras, $K - [12]$ colour as a function of the pulsation amplitude at K , ΔK . Symbols as in Fig. 1.

tic C stars under discussion. We omit four stars classed by Whitelock et al. as C-rich: WBP14 for which the data were uncertain; 04496–6958 and SHV 05210–6904, which lie above the PL relation (Whitelock et al. suggested that this may be the result of extra energy from hot bottom burning, although that conclusion is controversial for a carbon star and more detailed studies are required to investigate these luminous stars); 05128–6455 which Matsuura et al. (2005) have shown to be O-rich. Thus we have 38 C-rich Miras which are illustrated in a PL diagram (Fig. 6), for which a least squares fit gives:

$$M_{bol} = -2.54 \log P + 1.87, \quad (\sigma = 0.17) \quad (1)$$

assuming that the distance modulus of the LMC is 18.50 mag. This is close to the relationships given in the various references cited above and is what we use in Section 9 to derive distances. Some of the 0.17 mag dispersion will be introduced by the limited temporal coverage of IRAS (the satellite did not observe long enough to provide mean magnitudes for these long period stars).

This PL is distinctly different from that derived for O-rich Miras (Feast et al. 1989; Whitelock et al. 2003). Due to the differences in slope the relations, which are close at short periods, diverge at long period. At a period of 500 days the C-Miras are 27 percent fainter than their O-rich counterparts at the same period. Part of this difference may be due to the different energy distributions of the O- and C-rich stars which can lead to different systematic errors affecting the estimates of total luminosity (e.g. the strong water features which are present in O-rich, but not C-rich Miras). However, the large differences at long periods suggest that there may be real luminosity differences between the two types of Mira at a given period.

The PL relationship is revisited in Paper III of this series, where the kinematics of the Galactic C Miras are used to derive a zero-point.

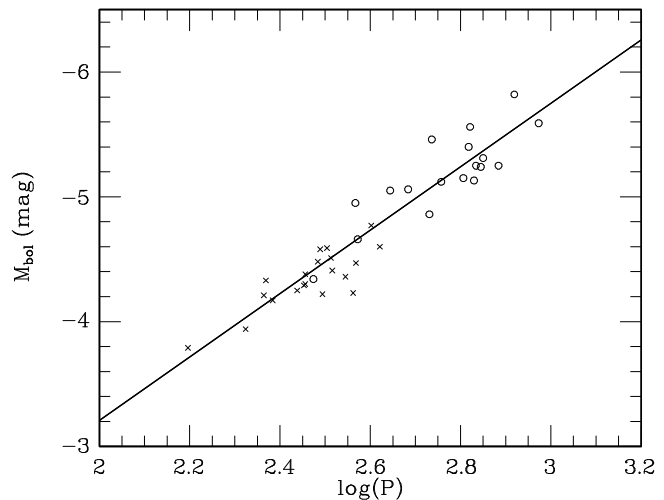


Figure 6. The PL relation for C-rich Miras in the LMC. The crosses and circles represent stars from Feast et al. (1989) and from Whitelock et al. (2003), respectively. The straight line is the locus given by equation 1.

6 INFRARED COLOURS

In the following analysis we compare various data on Galactic C-rich Miras with comparable measurements of LMC objects. The LMC samples are taken from Feast et al. (1989) (with updated periods from Glass & Lloyd Evans (2003)) and Whitelock et al. (2003). Note that the Feast et al. stars, which were optically selected, do not have L or IRAS observations; many of the Whitelock et al. sample, which were selected from IRAS sources, do not have J measurements; thus not all the stars appear in all the diagrams. Two bright LMC C stars with distinctly blue colours for their period are always distinguished in the illustrations. These stars, which also lie above the bolometric period-luminosity relation, are thought to be undergoing hot bottom burning (Whitelock et al. 2003).

Figs. 7 and 9 illustrate the colours prior to correction for reddening. The stars illustrated here are those with 10 and 20 classifications in Table 2 and with at least 9 observations contributing to the mean. Thus they represent well-characterized *normal* Miras and non-Miras as far as it is possible to define them.

It is clear that the Miras spread to much redder colours than the non-Miras as one might expect given their higher mass-loss rates and resultant circumstellar shells. At the blue extreme the non-Miras and Miras follow slightly different loci in the two-colour diagrams, but the differences are subtle and it is not possible to distinguish between individuals in the two groups simply on the basis of their colours. This is in marked contrast to the situation for O-rich stars (e.g. Whitelock et al. 1995).

The lines illustrated in these two figures represent a maximum likelihood fit to the Mira data and are given in equations 7 and 8, which are discussed later.

The reddening-corrected colours for the Miras only are illustrated in Figs. 8 and 10 where they are compared to the colours of Miras in the LMC (the derivation of the reddening corrections is given in Section 9, below). The colours of the Miras with peculiarities (class 1n, $n=1,5$), which are il-

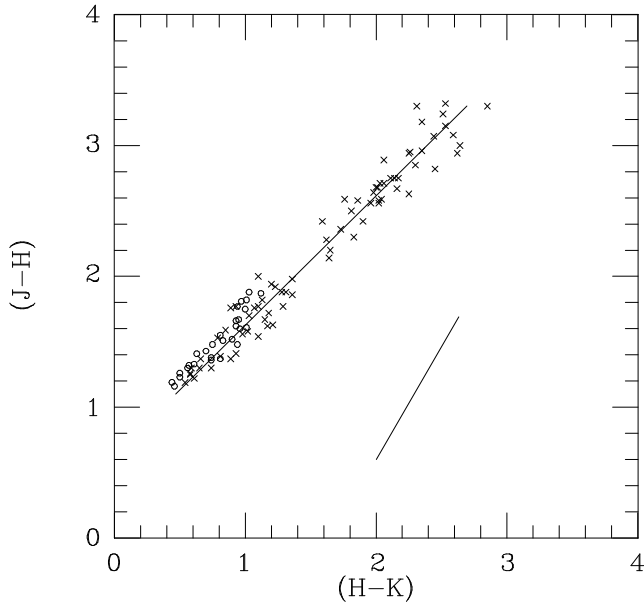


Figure 7. A two-colour diagram comparing Miras (crosses) having known periods, with non-Miras (open circles); stars from both groups are well observed (at least 9 measurements) and lack obvious peculiarities. The locus for the Miras, given in equation 7, is illustrated as is a reddening vector for $A_V = 10$ mag.

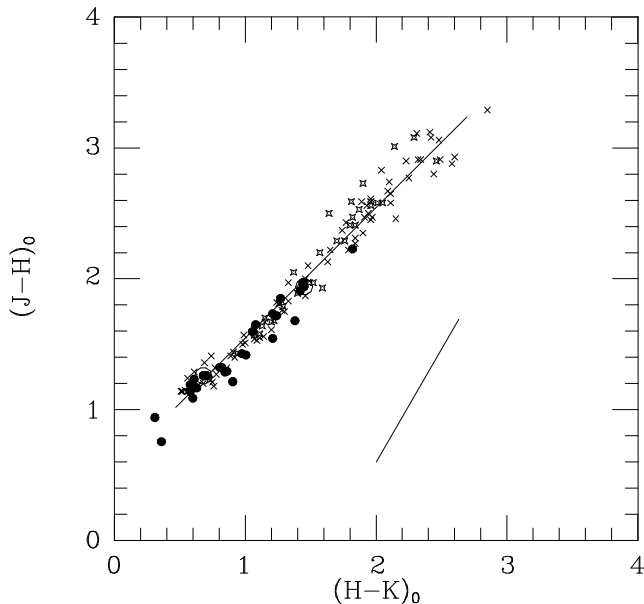


Figure 8. As Fig. 7, but after correcting for interstellar extinction as described in section 9 and showing only the Miras, but including those with peculiarities (open crosses). The filled circles are the LMC Miras, with the two large open circles representing LMC stars suspected of undergoing hot bottom burning.

illustrated as open crosses, do not differ significantly from the class 10 Miras. The loci illustrated in the two figures were fitted by maximum likelihood to the class 10 objects only:

$$(H - K)_0 = -0.549 + 1.002(J - H)_0, \quad (\sigma = 0.010), \quad (2)$$

$$(K - L)_0 = -0.252 + 1.295(H - K)_0, \quad (\sigma = 0.014), \quad (3)$$

Note that the J values for some of the faint LMC sources

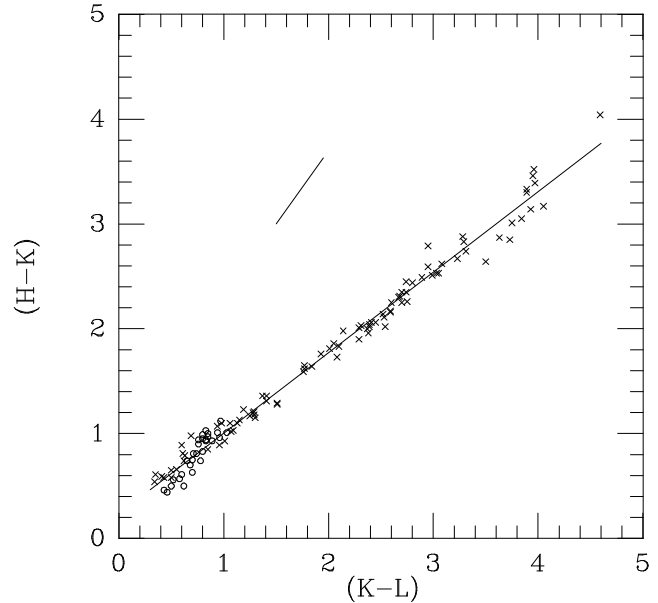


Figure 9. As Fig. 7, but for alternative colours. The locus described by equation 8 is shown.

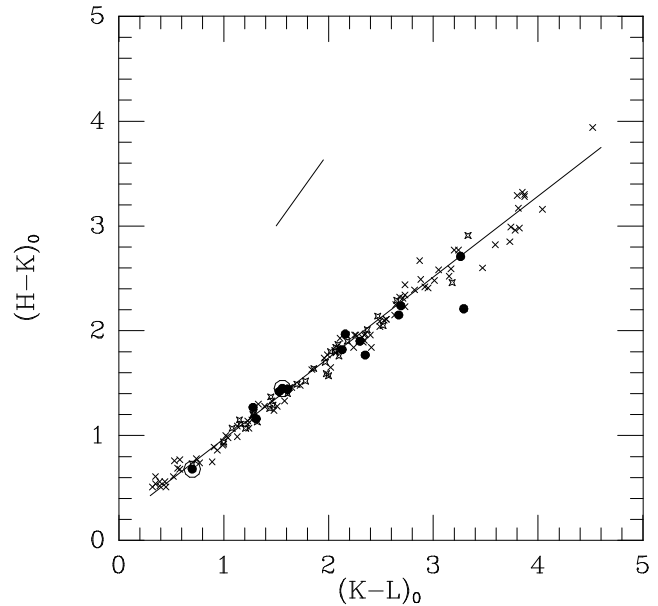


Figure 10. As Fig. 9, but after correcting for interstellar extinction as described in section 9 and showing only the Miras; the symbols are as in Fig. 8.

in Fig. 8 are uncertain by up to 0.2 mag, as are the H values for the faintest LMC sources in Fig 10. There appears to be a small shift between the LMC and the Galactic JHK colours in that $(J - H)$ for the LMC sources is on average ≤ 0.1 mag less for the LMC stars than for the Galactic ones at the same $(K - L)$. Cohen et al. (1981) discuss a colour difference between Galactic and LMC C-stars in the same sense, but few of their sample are Miras and their stars are in the colour range $0.4 < (H - K)_0 < 0.8$. For $(H - K)_0 < 0.8$ we find that LMC and Galactic C-rich Miras occupy the same part of the two-colour diagram. This diagram is obviously rather sensitive to reddening corrections and to errors in transfor-

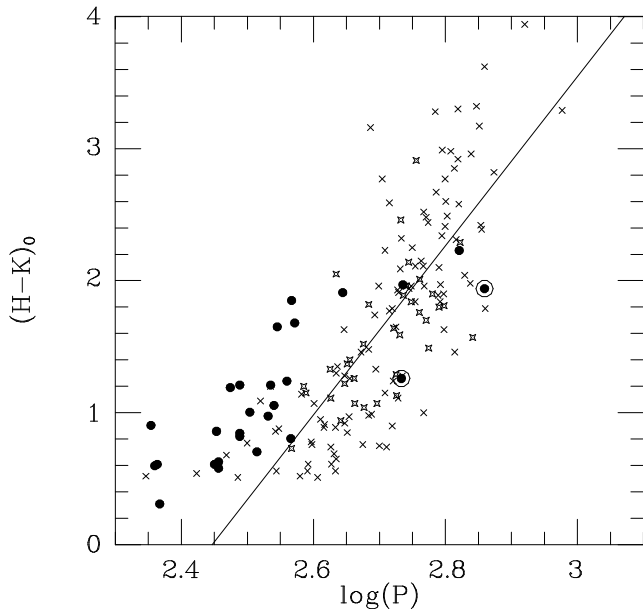


Figure 11. Period $(H - K)$ colour relationship for Galactic (crosses) and LMC (closed circles) C stars. The open crosses represent Galactic Miras with $\ln(n > 1)$ classifications. The two LMC points with circles around them are luminous Miras thought to be undergoing hot bottom burning. The locus described by equation 4 is shown.

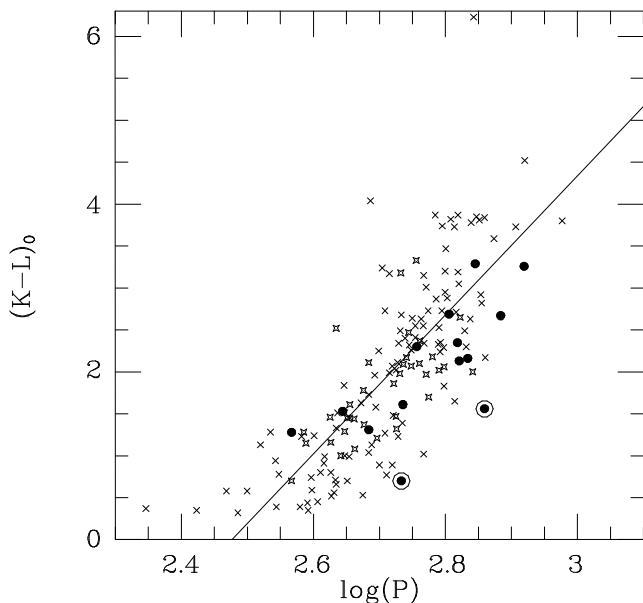


Figure 12. Period $(K - L)$ colour relationship with symbols as in Fig 11. The locus described by equation 5 is shown.

mation between different photometric systems, which tend to be largest for J .

The Galactic $(H - K)_0$ and $(K - L)_0$ period-colour relationships are compared to those for Miras in the LMC in Figs. 11 and 12. There is no obvious difference between the class 10 and class 1n ($n > 1$) Miras. There appear to be differences between the distributions of LMC and Galactic Miras in these figures, but there is a great deal of overlap between the two samples and the differences could plausibly

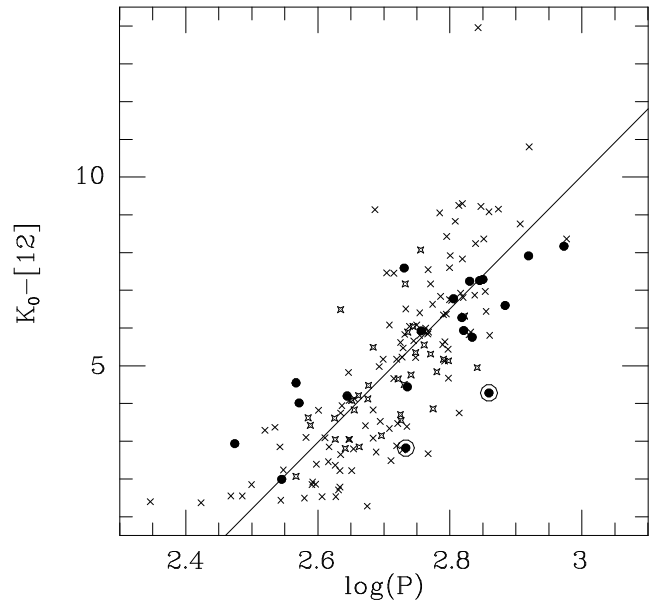


Figure 13. $K - [12]$ as a function of period for all of the Miras (class 1n) discussed here, compared with C stars from the LMC (closed circles) C stars. The two LMC points with rings around them are luminous Miras thought to be undergoing hot bottom burning. The locus described by equation 6 is shown.

be attributed to the very different selection effects in the Galactic and LMC samples. In particular it is possible that we would have been unable to measure the H flux for any LMC Miras with extremely red colours ($H - K > 2.8$). It is also likely that our selection criteria for the Aaronson and for the IRAS samples would have excluded most short period Miras. The relatively blue $(H - K)$ and $(K - L)$ colours of the Galactic Miras, compared to the LMC ones, with periods less than 500 days is notable.

Although neither $H - K$ nor $K - L$ shows a linear dependence on period there is certainly a trend to larger colours at longer period. The least-squares fit to the Galactic data in Figs. 11 and 12 (omitting the points at the shortest period, SZ Ara, in both figures and the one with the largest $K - L$, LL Peg, in Fig. 12) gives the following relationships:

$$(H - K)_0 = -15.69 + 6.412 \log P \quad (\sigma = 0.48), \quad (4)$$

and

$$(K - L)_0 = -20.56 + 8.300 \log P \quad (\sigma = 0.61). \quad (5)$$

Fig. 13 shows $K - [12]$ as a function of period and compares it to LMC data. The straight line is a least squares fit to the Galactic data, which yields:

$$K_0 - [12] = -43.0 + 17.7 \log P \quad (\sigma = 1.5) \quad (6)$$

$K - [12]$ is a very good indicator of the optical depth of the dust shell and hence of the dust mass-loss rate (e.g. Whitelock et al. 1994). There has been some discussion in the literature of differences in mass-loss rates between the Magellanic Clouds and the Galaxy. Such differences might be expected if Magellanic Cloud Miras have lower metallicity than their Galactic counterparts and therefore form dust with lower efficiency. If, however, the pulsation period of the Mira is a function of its metallicity, as it is for O-rich Miras (Feast & Whitelock 2000), differences between

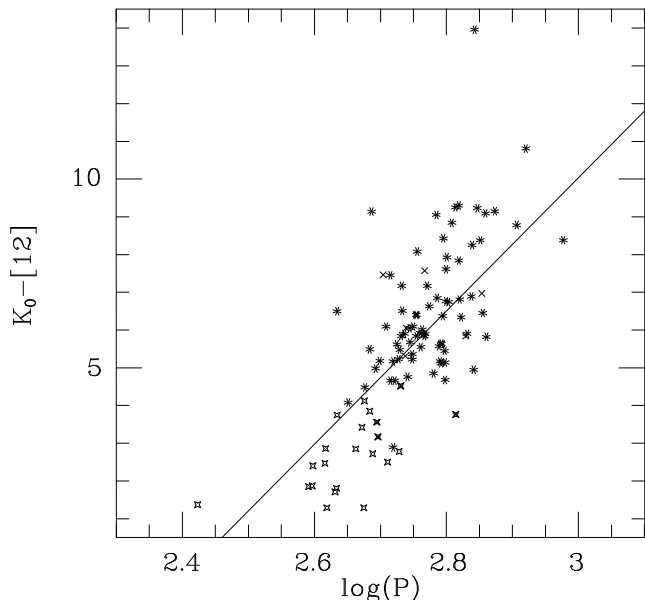


Figure 14. As Fig. 13 but showing only stars from the IRAS sample (asterisks), the faint IRAS sample (crosses) and the Aaronson sample (open crosses); note that four of the Aaronson sample are also faint IRAS sources. The line is equation 6.

the two systems will be more subtle. A recent analysis by van Loon (2006) suggests that, while the situation is very complex, there is no evidence for a mass-loss rate dependence on metallicity. The differences seen in Fig. 13 seem to be relatively minor and may be due to selection effects in the various samples rather than to fundamental properties of the two galaxies.

The very large effect of selection criteria is well illustrated by Fig. 14 which shows only the Galactic C stars, but distinguished according to the original sample from which they were drawn. Note that there is almost no overlap between the bright IRAS selected stars, most of which have $K - [12] \geq 5$ mag, and the optically selected Aaronson sample which all have $K - [12] \leq 5$ mag. It is clear that the C Miras show a large range of colour at a given period and that selection criteria will determine how this range is sampled.

7 APPARENT BOLOMETRIC MAGNITUDES

The bolometric magnitude was calculated by spline fitting to the $JHKL$, 12 and 25 μm flux as a function of frequency, as described in Section 6 of Whitelock et al. (1994) and/or by spline fitting to $JHKL$ MSX- A flux in the same way.

Some preliminary tests were done to compare the results of using spline fits to $JHKL$ and MSX- A , - C and - D fluxes with those on $JHKL$ and MSX- A . This because there were only 67 stars with the full data set. These tests indicated that a small colour correction was necessary if the integrations using only MSX- A were to give the same result as the full dataset. Thus the bolometric magnitudes derived by spline fitting $JHKL$ and MSX- A were corrected by $0.0119 - 0.0148 \times (K - L)$; its largest effect is to change the bolometric magnitude by only -0.055 mag.

There were 91 Miras with both MSX- A and IRAS data and the mean difference in the bolometric magnitudes de-

rived from the two sets (IRAS-MSX) was -0.02 ± 0.03 mag, with extreme values of -0.73 and $+0.35$. The corrections with the largest absolute values were always for the redder sources, as the mid-infrared is less important for the bluer sources.

Where there is no value for J (24 stars), H (3 stars) or L (1 star) an estimate is made from one of the following relations, for the purpose of calculating the bolometric magnitude:

$$(H - K) = -0.642 + 1.011(J - H), \quad (7)$$

$$(H - K) = +0.233 + 0.769(K - L). \quad (8)$$

These loci are illustrated in Figs. 7 and 9. If the 12 μm flux has been measured, but the 25 μm flux has not, the colour corrected [25] is estimated from:

$$([12] - [25])_{cc} = 0.0337 + 0.109(K - [12]). \quad (9)$$

Because it is only for very red stars that J or H were not measured, and only for blue ones that [25] was not measured, these estimates do not compromise the quality of the final bolometric magnitude. The L flux is much more important, but only one Mira with a known period, CF Cru, does not have a measured value for L , which is estimated from H via equation 8 above.

Given that we chose to reject the faint cycles for the very well observed stars we examine briefly the difference it would make to the bolometric magnitudes if we used faint rather than bright cycles, assuming that the cause of the change is line of site obscuration and that the IRAS and/or MSX fluxes remain constant. R For would go from $m_{bol} = 4.54$ to 4.97, R Lep from $m_{bol} = 3.52$ to 4.13 and II Lup from $m_{bol} = 3.89$ to 4.07, the size of the change being strongly dependent on the relative contributions to the total flux from $JHKL$ and from the mid-infrared.

8 BOLOMETRIC CORRECTIONS

The main interest in bolometric corrections is their use when limited data are available. With this in mind we provide, in Table 5, the coefficients of the best fit least squares fourth order polynomials to the bolometric correction at K , BC_K as a function of the colour ($x - y$):

$$BC_K = c_0 + c_1(x - y) + c_2(x - y)^2 + c_3(x - y)^3 + c_4(x - y)^4, \quad (10)$$

for a variety of colours. The table also includes the maximum (max) and minimum (min) values of the colour for which the fit was determined (this type of fit should not be extrapolated), the error (σ) associated with an individual observation and the number of stars used in the fit (No).

Two examples of these fits are shown in Fig. 15 for $(J - K)_0$ and $K_0 - [12]$. It is clearly possible to derive an accurate bolometric correction if observations in widely separated bands, such as K and [12], are available. In practice it will often only be possible to use something like $(J - K)$ when dealing with photometry from e.g. the 2MASS survey or typical measurements that are now being done on extragalactic C stars with large telescopes.

The curves listed in Table 5 provide excellent fits to the LMC C-star bolometric corrections discussed by Whitelock et al. (2003) and illustrated in their fig. 13, although

Table 5. Coefficients for calculating the bolometric correction as a function of colour according to equation 10.

	$(J - K)_0$	$(H - K)_0$	$(K - L)_0$	$(K - [12])_0$	$(K - A)_0$
c_0	0.972	2.360	3.228	2.801	3.130
c_1	2.9292	3.1729	0.8720	0.7101	0.4807
c_2	-1.1144	-2.5747	-0.7042	-0.1958	-0.1655
c_3	0.1595	0.5462	0.06350	0.01032	0.002241
c_4	-9.5689×10^{-3}	-0.043014	-1.6341×10^{-3}	-2.2054×10^{-4}	-2.2405×10^{-4}
max	6.5	4.0	6.2	14	10
min	1.5	0.5	0.3	1.2	0.5
σ	0.23	0.27	0.17	0.11	0.13
No.	123	142	144	144	70

the LMC data do show more scatter because the stars are fainter. There is no evidence of any difference between C stars in the Galaxy and the LMC in respect of the bolometric corrections as a function of colour.

The lack of scatter in Fig. 15 is largely a consequence of the way the bolometric magnitudes are calculated. Thus, for example, if we examine II Lup during a bright cycle ($\bar{K} = 1.79$ mag) we derive $K - [12] = 5.92$ and $BC_K = 2.15$, while during a faint cycle ($\bar{K} = 3.0$ mag) we obtain $K - [12] = 7.12$ and $BC_K = 1.2$; both of these points fit on the curve in Fig. 15. The bolometric magnitude derived from these data, $m_{bol} = 0.48$ and 0.52 , are not very different because the $JHKL$ flux is only a small part of the total. In contrast, for R Lep we obtain $K - [12] = 2.81$ and $BC_K = 3.47$ when it is bright ($\bar{K} = 0.07$ mag) and $K - [12] = 3.54$ and $BC_K = 3.36$ when it is faint ($\bar{K} = 0.8$ mag). Again the points fall close to the curve in Fig. 15, but the resulting bolometric magnitudes, $m_{bol} = 3.52$ and 4.13 , differ considerably because the $JHKL$ flux is a major contributor to the total.

Fig. 15 also shows a comparison with the bolometric correction derived by Guandalini et al. (2005) for a slightly different colour ($K - [12.5]$). The two relations differ by at most 0.19 mag in the region in which there are many points, $3 < K - [12] < 4$, and this difference goes up to 0.36 mag at $K - [12] = 14$.

9 INTERSTELLAR REDDENING AND DISTANCES

We assume that the Galactic C-rich Miras obey the LMC bolometric PL relation as discussed above (Section 5). Thus a first estimate can be made of the distance to the star by comparing the measured and absolute bolometric magnitudes. The extinction is then estimated using the Drimmel et al. (2003) three dimensional Galactic extinction model, including the rescaling factors that correct the dust column density to account for small scale structure seen in the DIRBE data, but not described explicitly by the model. The measured mean $JHKL$ magnitudes are corrected for extinction following the reddening law given by Glass (1999) and the bolometric flux is recalculated. This process of calculating distance, extinction and bolometric magnitude is then iterated as necessary, typically two to five times, until the distance modulus changes by less than 0.01 mag. The extinction values, A_V , derived in this way are listed in Table 6.

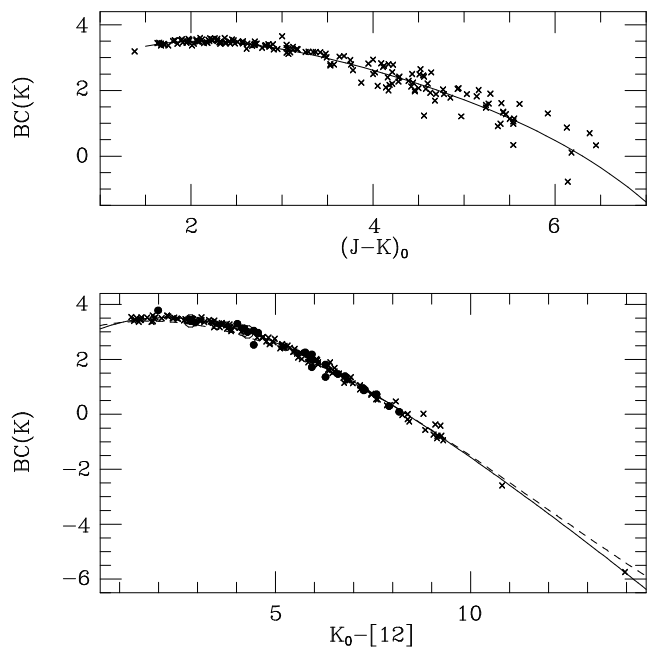


Figure 15. The bolometric correction at K as a function of (top) $(J - K)_0$ and (bottom) $K_0 - [12]$. The curves are fourth order polynomials with the parameters given in Table 5. The lower figure also shows LMC values (solid circles) from Whitelock et al. (2003). The dashed curve is the relation for $K - [12.5]$ from Guandalini et al. (2005) fig. 5.

They range up to $A_V \sim 5.8$ and therefore have a significant effect on the $JHKL$ colours and on the derived distances.

We have 70 stars in common with those of Groenewegen et al. (2002) for which the derived distances can be compared. Groenewegen et al. calculate distances either from the PL relation of Groenewegen & Whitelock (1996), for stars with known periods longer than 390 days, or from the $12 \mu\text{m}$ flux, with a bolometric correction that depends on the 25 to $12 \mu\text{m}$ flux ratio, for the others. The statistical agreement is good, with the average distance calculated by Groenewegen et al. for the 70 stars in common being only 8 percent larger than our value.

Table 6: Derived data for Miras with pulsation periods.

name	dist (kpc)	A_V	m_{bol}	$(J - H)_0$	$(H - K)_0$ (mag)	$(K - L)_0$	$K_0 - [12]$	K_0	$\log \dot{M}$ ($M_\odot \text{yr}^{-1}$)	BC_K (mag)
YY Tri	2.25	0.24	6.53		2.99	3.74	8.43	6.79	-4.45	-0.26
R For	0.70	0.04	4.54	1.67	1.20	1.28	3.62	1.21	-5.87	3.33
[TI98]0418+0122	6.42	0.37	9.24	1.83	1.33	1.46	3.61	5.98	-5.73	3.26
V718 Tau	1.46	1.35	6.12	1.70	1.15	1.15	3.42	2.72	-5.85	3.41
R Lep	0.47	0.25	3.52	1.43	0.94	1.00	2.81	0.05	-6.03	3.47
QS Ori	2.65	0.69	7.17	1.50	0.98	1.04	3.08	3.74	-5.89	3.43
05418-3224	2.73	0.04	7.24	2.47	1.82	2.11	5.49	4.86	-5.19	2.38
06088+1909	2.37	1.18	6.91	2.37	1.74	1.96	4.98	4.15	-5.08	2.76
ZZ Gem	1.76	0.61	6.75	1.32	0.77	0.58	1.85	3.15	-6.65	3.60
V617 Mon	2.94	1.01	7.48	1.68	1.22	1.29	3.05	4.08	-5.96	3.41
V636 Mon	1.09	0.45	5.11	1.83	1.28	1.39	3.39	1.78	-5.76	3.34
V477 Mon	2.61	1.01	6.86	2.31	1.84	2.24	5.12	4.46	-4.83	2.40
RT Gem	3.43	0.54	8.08	1.24	0.56	0.39	1.44	4.57		3.51
06487+0551	2.40	0.80	6.84	2.47	1.91	2.34	5.47	4.55	-5.36	2.29
CG Mon	1.99	0.75	6.69	1.29	0.61	0.52	1.53	3.23		3.46
CL Mon	1.11	0.47	5.22	1.67	1.15	1.27	3.34	1.84	-5.85	3.38
06531-0216	2.01	0.86	6.35	1.97	1.49	1.70	3.86	3.27		3.07
06564+0342	2.99	0.83	7.24	2.58	2.11	2.55	5.84	5.35	-5.27	1.89
07080-0106	3.76	0.16	7.70	2.80	2.44	2.73	6.63	6.22	-4.71	1.48
VX Gem	1.88	0.03	6.66	1.22	0.61	0.35	1.92	3.13	-6.54	3.53
R Vol	0.88	0.49	4.84	1.89	1.40	1.61	3.83	1.67	-5.70	3.18
HX CMa	1.68	0.74	5.73	2.38	1.79	2.17	5.81	3.55	-4.90	2.18
07217-1246	2.18	0.84	6.47	2.47	1.97	2.35	5.64	4.22	-4.98	2.24
07220-2324	2.75	1.13	7.09	2.59	1.96	2.26	5.22	4.67	-5.22	2.42
[W71b]007-02	4.34	1.33	8.29	1.62	1.07	1.08	2.85	4.81		3.49
07373-4021	1.09	0.54	5.30	1.81	1.26	1.44	4.21	2.18	-5.51	3.12
V471 Pup	4.17	1.43	8.39	1.14	0.56	0.44	1.85	5.00		3.39
07454-7112	0.83	0.45	4.60	2.90	2.23	2.73	6.08	2.78	-5.14	1.82
V831 Mon	2.33	0.09	7.31	1.53	1.09	1.13	3.29	3.88	-6.05	3.43
07576-4054	2.86	1.25	7.26		2.59	3.17	7.45	6.51	-5.18	0.75
07582-1933	2.49	0.44	6.91	2.91	2.32	2.68	6.51	5.35	-5.02	1.56
[ABC89]Pup38	12.30	0.98	10.63	1.75	1.30	1.33	3.75	7.34		3.29
FF Pup	3.77	0.58	8.06	1.20	0.65	0.66	2.65	4.64		3.42
V518 Pup	2.03	0.10	6.67	2.05	1.37	1.45	4.08	3.51	-5.68	3.16
08050-2838	2.63	0.97	7.01	3.01	2.14	2.47	6.04	4.99	-5.10	2.01
08074-3615	2.40	1.52	6.37		3.94	4.52	10.80	8.95	-4.32	-2.59
[ABC89]Ppx19	5.89	2.19	8.93	1.97	1.52	1.78	4.12	5.91		3.01
V346 Pup	1.36	0.88	5.57	2.65	2.11	2.55	6.40	3.67	-4.85	1.90
[ABC89]Ppx40	5.13	1.54	8.74	1.36	0.69	0.56	1.71	5.22		3.52
[W71b]029-02	4.88	3.04	8.53	1.87	1.46	1.63	3.41	5.35		3.17
08340-3357	2.26	0.83	6.60	3.06	2.48	3.01	7.17	5.53	-4.84	1.07
R Pyx	1.35	0.38	6.00	1.23	0.73	0.70	2.07	2.50	-6.38	3.50
UW Pyx	1.50	0.67	6.11	1.34	0.74	0.80	2.36	2.62	-6.28	3.49
08535-4724	3.51	4.53	7.64		2.91	3.33	8.07	7.17	-4.53	0.47
08534-5055	4.29	2.20	7.90		3.32	3.85	9.22	8.30	-4.24	-0.40
IQ Hya	1.55	0.53	6.26	1.56	1.14	1.23	3.10	2.84	-6.05	3.42
CQ Pyx	1.14	0.49	4.99		3.30	3.87	9.30	5.94	-4.76	-0.94
09176-5147	3.17	3.64	7.69	2.58	2.05	2.52	6.49	5.98	-4.77	1.71
[W71b]046-02	5.12	5.63	9.26	1.15	0.54	0.35	1.37	5.87		3.40
[ABC89]Vel44	4.18	3.34	8.33	1.41	0.89	0.91	2.46	4.85		3.48
09433-6233	8.66	0.90	9.60	2.29	1.70	1.97	5.31	7.10	-5.02	2.50
CW Leo	0.14	0.07	0.40	3.29	2.85	3.73	9.25	1.18	-4.65	-0.78
09513-5324	1.79	1.87	6.05	3.12	2.41	2.95	6.75	4.90	-4.82	1.15
09529-5506	2.80	1.82	6.90	2.55	1.98	2.63	6.87	5.65	-4.69	1.25
09533-6021	4.81	1.48	8.03	3.08	2.42	2.92	6.97	6.90	-4.74	1.14
09521-7508	1.12	0.72	5.19	2.67	2.09	2.49	5.83	3.15	-5.19	2.03
09586-6150	9.13	1.03	9.80		2.77	3.24	7.46	9.10	-4.75	0.71

Continued on Next Page...

name	dist (kpc)	A_V	m_{bol}	$(J - H)_0$	$(H - K)_0$ (mag)	$(K - L)_0$	$K_0 - [12]$	K_0	$\log M$ ($M_\odot yr^{-1}$)	BC_K (mag)
10026-5849	5.68	4.73	8.72	1.79	1.29	1.47	3.71	5.47		3.25
10098-5742	3.91	3.54	7.81		2.52	3.15	7.55	7.23		0.58
10109-5958	2.95	1.70	7.55	1.58	1.11	1.16	3.05	4.12		3.43
RW LMi	0.46	0.09	3.10	2.74	2.10	2.53	6.35	1.31	-4.94	1.78
10199-5801	4.39	4.33	7.90	2.83	2.04	2.49	5.82	5.81	-4.10	2.09
10220-5858	5.45	3.73	8.52	1.51	1.00	1.02	2.67	5.05		3.47
CPD-58 2175	5.76	4.53	8.72	2.45	1.96	2.40	6.04	6.73		1.99
CZ Hya	1.35	0.13	5.80	1.40	0.92	1.00	3.05	2.38	-6.06	3.42
TV Vel	1.84	1.08	6.57	1.14	0.51	0.45	1.53	3.14		3.43
[ABC89]Car73	6.05	4.52	8.97	2.10	1.48	1.73	3.83	5.93		3.04
[ABC89]Car84	4.54	4.45	8.30	1.21	0.75	0.89		4.93		3.36
[ABC89]Car87	7.09	3.46	9.33	1.18	0.76	0.53	1.28	5.81		3.53
[ABC89]Car105	2.95	2.57	7.37	1.57	1.07	1.21	3.15	4.01		3.36
11145-6534	1.73	1.51	5.96	2.91	2.34	2.73	6.37	4.35	-4.82	1.61
[W65] c13	5.38	4.53	8.93	1.27	0.78	0.74	1.86	5.44		3.49
[TI98]1130-1020	2.16	0.09	6.82	2.13	1.63	1.84	4.82	4.03	-5.56	2.79
11318-7256	0.66	0.56	4.07	1.82	1.24	1.48	3.47	0.80	-5.66	3.27
[ABC89]Cen4	4.00	1.68	8.00	1.41	0.74	0.77	2.49	4.53		3.47
11463-6320	3.13	2.77	7.27	2.59	1.89	2.33	5.56	5.19	-4.84	2.08
[ABC89]Cen32	4.40	2.58	7.94	2.00	1.46	1.65	3.75	4.82	-5.45	3.12
[ABC89]Cen43	6.06	3.93	8.85	1.55	1.11	1.23	2.77	5.46		3.39
[ABC89]Cen60	5.25	3.50	8.82	1.44	0.91	0.99	2.85	5.39		3.43
CF Cru	5.88	5.80	9.03	1.14	0.56		1.79	5.68		3.35
12194-6007	2.84	2.21	7.04	2.35	1.90	2.29	5.44	4.76	-5.21	2.28
12298-5754	1.85	1.58	6.19	2.46	2.15	2.63	6.00	4.26	-4.86	1.93
CGCS3268	2.05	1.36	6.83	1.20	0.76	0.59	2.39	3.31		3.52
12394-4338	1.33	0.34	5.53	2.56	1.96	2.17	4.76	2.88	-5.41	2.65
12421-6217	4.87	5.42	8.03			3.73	8.76	7.98	-4.24	0.06
RU Vir	0.91	0.08	4.94	1.76	1.28	1.51	4.08	1.79	-5.69	3.15
V Cru	1.47	0.98	6.16	1.14	0.52	0.39	1.49	2.79		3.37
12540-6845	1.37	0.65	5.52	2.61	1.96	2.34	5.89	3.46	-4.71	2.06
13343-5807	2.40	1.94	6.82	2.50	1.94	2.32	5.66	4.80	-5.14	2.01
13477-6532	2.32	1.36	6.49		2.96	3.78	8.24	6.50	-4.52	-0.01
13482-6716	1.70	0.87	6.17	2.59	1.96	2.25	5.17	3.70	-5.20	2.47
13509-6348	2.98	2.30	7.06			2.30	5.89	4.91	-5.16	2.15
[ABC89]Cir26	3.81	4.11	7.93	1.97	1.33	1.58	3.53	4.75		3.18
[ABC89]Cir27	3.57	4.14	7.70	1.93	1.59	1.98	4.50	4.89	-5.35	2.80
14395-5656	6.58	3.41	9.13	1.57	0.99	1.13	2.71	5.70		3.43
14404-6320	3.62	2.55	7.53		2.98	3.82	8.83	8.09	-4.75	-0.55
14443-5708	5.17	3.43	8.27		3.62	3.84	9.08	8.62	-4.15	-0.35
15082-4808	0.95	0.60	4.65	2.93	2.60	3.47	7.92	4.31	-4.67	0.35
15084-5702	3.48	3.58	7.05		3.29	3.80	8.36	7.00	-4.10	0.04
II Lup	0.64	0.48	3.89	2.29	1.76	2.10	5.92	1.75	-4.82	2.15
15261-5702	3.31	1.51	7.23		2.40	2.82	6.44	5.82	-4.72	1.41
16079-4812	2.13	3.36	6.28		3.18	3.82	8.36	6.54	-4.69	-0.26
NP Her	2.44	0.17	7.07	1.41	0.85	0.70	2.22	3.48	-6.37	3.59
16171-4759	2.84	2.70	7.16	2.40	1.83	2.07	5.35	4.64		2.52
V Oph	0.78	0.90	5.06	1.20	0.68	0.58	1.55	1.53	-6.95	3.53
CGCS3721	2.71	1.29	7.56	1.34	0.88	0.78	2.24	4.00		3.56
16538-4633	2.42	2.57	6.88	2.49	1.64	1.85	4.65	4.04	-4.67	2.84
16545-4214	1.03	0.75	5.01	2.56	1.93	2.11	5.23	2.45	-5.02	2.56
17047-2848	3.22	1.31	7.49	2.22	1.65	2.02	5.62	5.24	-5.07	2.25
V2548 Oph	1.09	0.87	4.75		2.82	3.59	9.15	5.53	-4.47	-0.78
SZ Ara	2.44	0.47	7.84	1.11	0.52	0.37	1.40	4.41	-6.48	3.44
V617 Sco	1.29	1.19	5.52	1.39	0.91	0.89	2.88	2.06		3.46
17105-3746	2.73	3.20	7.07	2.23	1.82	2.40	5.81	4.85	-4.75	2.22
17130-3907	2.24	1.62	6.52	2.59	1.82	2.07	5.13	4.08	-4.90	2.44
17217-3916	2.88	2.03	7.10		2.75	3.19	7.60	6.24		0.86
17222-2328	2.64	2.58	6.92	2.73	1.90	2.18	4.84	4.37	-5.14	2.55

Continued on Next Page...

name	dist (kpc)	A_V	m_{bol}	$(J - H)_0$	$(H - K)_0$ (mag)	$(K - L)_0$	$K_0 - [12]$	K_0	$\log M$ ($M_\odot yr^{-1}$)	BC_K (mag)
V833 Her	1.07	0.14	5.08	2.90	2.46	3.18	7.17	4.18	-4.68	0.91
17446-4048	1.40	0.80	5.66	2.52	1.89	2.09	5.89	3.53	-5.06	2.13
17463-4007	10.55	1.22	10.38	1.54	1.07	1.24	3.82	7.11		3.27
17581-1744	2.34	1.72	6.62	2.30	1.63	1.83	4.67	3.87	-5.25	2.75
18036-2344	2.25	2.61	6.47	3.06	2.28	2.64	6.32	4.69	-4.59	1.78
FX Ser	1.13	1.39	5.25	2.43	1.77	1.99	4.66	2.46	-5.12	2.78
V1280 Sgr	1.34	1.03	5.59	1.64	1.13	1.32	3.55	2.30	-5.71	3.29
18119-2244	2.21	1.67	6.54		2.68	2.87	6.84	5.45	-4.78	1.09
V5104 Sgr	1.05	0.63	4.82	3.11	2.31	2.71	6.92	3.46	-4.70	1.36
18239-0655	1.74	1.64	5.96	2.90	2.49	2.88	6.73	4.49	-4.53	1.47
V1076 Her	1.14	0.36	5.07		3.28	3.87	9.05	5.81	-4.64	-0.73
18248-0839	2.29	1.58	6.53	3.49	2.91	3.18	7.83	5.99	-4.56	0.54
V627 Oph	3.34	0.85	7.75	1.84	1.26	1.45	4.13	4.58	-5.59	3.16
V1417 Aql	0.87	0.36	4.49	2.41	1.80	2.02	5.17	1.93	-4.85	2.56
V821 Her	0.75	0.69	4.34	2.22	1.79	2.07	5.17	1.79	-5.36	2.55
V2045 Sgr	2.22	1.07	6.86	1.59	0.97	0.99	2.80	3.36	-5.98	3.50
AI Sct	2.15	1.06	6.90	1.50	0.95	0.80	3.09	3.38	-5.64	3.52
V1418 Aql	1.04	0.77	4.96	2.77	2.25	2.64	6.08	3.07	-4.90	1.89
V1420 Aql	1.00	0.52	4.66	2.20	1.57	2.00	4.95	2.03	-5.04	2.62
V1965 Cyg	1.13	0.56	5.11	2.58	2.01	2.37	5.55	2.90	-4.89	2.21
R Cap	1.62	0.46	6.45	1.32	0.86	0.94	2.85	3.01	-6.57	3.45
BD Vul	2.22	0.62	6.92	1.47	0.89	0.71	2.22	3.31	-6.14	3.60
V442 Vul	1.41	0.58	5.45	2.88	2.58	3.05	6.81	4.17	-4.82	1.29
RV Aqr	0.75	0.18	4.54	1.91	1.35	1.51	3.94	1.37	-5.71	3.17
[TI98]2259+1249	4.15	0.49	8.65	1.14	0.51	0.32	1.55	5.20	-5.88	3.45
LL Peg	1.05	0.09	4.75			6.23	13.96	10.49	-4.28	-5.74
IZ Peg	1.70	0.19	6.20		3.16	4.04	9.14	7.07	-4.86	-0.87
[TI98]2223+2548	2.84	0.16	7.69	1.61	1.20	1.28	3.37	4.34	-5.94	3.36

There are, however, some individually large differences and some systematic trends. For the bluer sources ($K - [12] < 6$) our distances tend to be smaller because the apparent bolometric flux we derive is larger and there is a clear trend with colour. The Groenewegen et al. results for the 34 stars with $K - [12] < 5.9$ are 24 percent more distant than we find. The most extreme case is R Cap (20084–1425), $K - [12] = 2.85$, for which we find 1.52 kpc while Groenewegen et al. get 3.45 kpc (Le Bertre et al. (2001) got 1.33 kpc; see below). The main source of this difference is in the apparent bolometric magnitudes, which differ by 1.25 mag, although the absolute magnitudes also differ in such a way as to increase the difference in derived distance. Our results suggest that Groenewegen et al. systematically underestimated the contribution from *HKL* to the total flux, thereby underestimating the apparent bolometric flux for blue sources. This will have had very little effect on the red sources that make up the bulk of their C-star sample.

For the redder sources our distances tend to be slightly larger than the Groenewegen et al. ones, but there is no systematic trend with colour for stars with $K - [12] > 6$ and the effect is not large. For the 36 stars with $K - [12] > 5.9$ Groenewegen et al. get distances 6.5 percent less than ours. The most extreme examples are RW LMi, $K - [12] = 6.35$, for which we and Groenewegen get 0.32 and 0.46 kpc respectively, and 08534–5055, $K - [12] = 9.22$, for which the distances are 3.10 and 4.29 respectively. For RW LMi the difference is entirely in the apparent bolometric magnitude and for 08534–5055 it is largely so.

Le Bertre et al. (2001) calculate distances using a [2.20–3.77] μm dependent bolometric correction to the [2.20] mag, applied to observations obtained with the Japanese IRTS. For this purpose they assume $M_{bol} = -5.01$ mag for all their sources (this is the bolometric magnitude we would associate with a Mira with a period of 530 days) indicating a factor of 1.8 uncertainty for the distances of individual sources owing to this latter assumption. They have only 3 sources in common with us, R Cap, HX Cma and 11318–7256, for which they estimate distances 9 to 30 percent smaller than we do.

CW Leo is a very well studied, thick-shelled, C star for which numerous distance estimates, in the range 0.11 to 0.17 kpc, have been made. It is also one of the few stars for which a geometric distance, of 0.145 kpc, has been measured using the dust outflow speed combined with the proper motion of the shell (Tuthill et al. 2000). This value is in good agreement with our estimate of 0.14 kpc.

Gundalini et al. (2005) tabulate distances (their tables 1 and 2) for various C stars including some Miras. For the four stars in common in their table 1 (which they describe as having “astrometric, or reliable, distance estimates”) their distances are, in the mean, 7 percent larger than ours. For the 8 stars listed in both our Table 5 and in their table 2, the mean difference is zero. The distances in table 1 of Gundalini et al. (2005), which are described as “astrometric” are taken from Bergeat & Chevallier (2005) and are based on a procedure of Knapik et al. (1998) who corrected the Hipparcos parallaxes by a semi-empirical statistical method of their own. Contrary to a standard Lutz-Kelker type approach to this problem, which would have resulted in negative corrections to the parallaxes and absolute magnitudes, both positive and negative corrections result from their method. They do not discuss the uncertainties in the corrections applied.

However, it is clear from table 1 of Bergeat et al. (1998) that these corrections are often large. Knapik et al. (1998) also say (their section 5), “: individual values [of the corrections] may occasionally be wrong and a few such cases were detected from data at hand..... In such cases the catalogue value can be kept if positive or the star is abandoned”.

So far as C-Miras are concerned, the possibility of using Hipparcos parallaxes to calibrate the zero-point of the PL(K) relation was investigated by Whitelock & Feast (2000). A definitive result was not obtained due primarily to the small number of C-Miras with parallaxes of significant weight. It may be possible to re-investigate this matter when the revision of the Hipparcos catalogue is completed (see van Leeuwen 2005, van Leeuwen & Fantino 2005).

The distances tabulated here probably represent the best currently available for carbon Miras, particularly for those where the light curve has been well characterized over many cycles. Noting the discussion in the last paragraph of Section 7 there is a potential problem in calculating accurate apparent bolometric luminosities during obscuration events (see also Section 11). If we had made *JHKL* observations of a C star with a thin dust shell (where most of the bolometric flux is emitted at near-infrared wavelengths) only during an obscuration event, then we would have underestimated its luminosity and overestimated its distance. It also remains possible that we have failed to identify a small number of bright hot-bottom-burning stars for which we will have underestimated the distances.

10 MASS-LOSS RATES

Mass-loss rates can be derived for many of these stars using the expression given by Jura (1987):

$$\dot{M} = 1.7 \times 10^{-7} v_{15} d_{kpc}^2 L_4^{-1/2} F_{\nu,60} \bar{\lambda}_{10}^{1/2} M_{\odot} \text{yr}^{-1}, \quad (11)$$

where v_{15} is the outflow velocity in units of 15 km s^{-1} , d is the distance in kpc, L_4 is the luminosity in units of $10^4 L_{\odot}$, $F_{\nu,60}$ is the flux from the dust at $60\mu\text{m}$ and $\bar{\lambda}$ is the mean wavelength of the light emerging from the star and its shell in units of $10 \mu\text{m}$. Note that this equation assumes a constant dust-to-gas ratio. The results are given in Table 6.

For the outflow velocity (v_{15}) we use the expansion velocities tabulated by Groenewegen et al. (2002) while noting that those authors, in their own calculation of mass loss add an additional drift velocity (of the order of 2 or 3 km s^{-1}) to their expansion velocities to determine the outflow velocity. For the stars in our sample which have no measured expansion velocity we assume 19 km s^{-1} , this being the mean for the 68 stars in our sample which have all the other parameters necessary to calculate \dot{M} . We find that $\bar{\lambda}$ varies from 0.23 to 1.42, i.e. it is generally somewhat larger than the 0.3 assumed by Groenewegen et al. particularly for the very red stars which constitute the bulk of their sample.

For $F_{\nu,60}$ we use the IRAS flux at $60\mu\text{m}$, and where there is no IRAS flux at this wavelength we do not attempt to calculate mass-loss rates. Note that this approach will result in an overestimate of the mass-loss rate if the shell is very thin and a significant fraction of the $60\mu\text{m}$ flux actually originates from the underlying star. We can estimate the effect by assuming the stars radiate as blackbodies at the temperatures given by Bergeat et al. (2002) and using

the K mag given in Table 6 to estimate the stellar contribution to the measured $60\mu\text{m}$ flux. Bergeat et al. tabulate temperatures for 4 of the 5 stars (none for R Cap) listed with $\log \dot{M} < -6.4 M_{\odot}\text{yr}^{-1}$ in Table 6. For V Oph, ZZ Gem, VX Gem and SZ Ara the stellar contribution to the $60\mu\text{m}$ flux will be approximately 39, 32, 23 and 12 percent, respectively. For these 5 stars (including R Cap, where the contribution from the star is estimated at 20 percent) the mass-loss rates given in the table have been adjusted by the amount indicated; for all the others the effect will be negligible.

For very close stars the $60\mu\text{m}$ flux will have been spatially resolved and therefore not entirely included in the IRAS PSC estimate. In which case the mass-loss rates would be underestimated. The 3 stars with distances under 500 pc are the only ones where the extended nature of the source is likely to be significant; these are CW Leo, R Lep and RW LMi. Two of these stars (CW Leo and R Lep) were examined by Young, Phillips & Knapp (1993) who found extended contributions from both, amounting to about 10 percent of the PSC flux. The mass-loss values tabulated for these three stars have therefore been increased by 10 percent. For all the other stars the effect will probably be insignificant, but certainly less than 10 percent.

A number of authors have calculated mass-loss rates for C-rich Miras and the results differ quite significantly from one paper to another. There are many factors which contribute to these differences, but uncertainty in the distance, which appears squared in equation 11, is always a major factor. This aspect has already been discussed in Section 9.

Whitelock et al. (1987) showed that mass-loss rates of relatively thin shelled O-rich Miras depended on their pulsation amplitudes, providing strong support for the role of pulsation in driving mass loss. While it would be very interesting to do a similar exercise for the C Miras under discussion, it is unfortunately not practical. As shown in Fig. 5 and discussed in Section 4.3 the $JHKL$ amplitudes tell us little about the pulsation amplitude of the star. Ideally we should measure the bolometric amplitude, but this must await monitoring at mid-infrared wavelengths.

Fig. 16 shows how the mass-loss rates depend on colour. The line is a polynomial fit to the Galactic C Miras:

$$\log \dot{M} = -7.668 + 0.7305(K - [12]) - 5.398 \times 10^{-2}(K - [12])^2 + 1.343 \times 10^{-3}(K - [12])^3. \quad (12)$$

The LMC Miras discussed by Whitelock et al. (2003) are shown for comparison. The two groups follow the same trend and the slight displacement of the LMC points with respect to the Galactic ones should not be seen as significant in view of the different assumptions that went into the mass-loss rate calculations (see van Loon et al. 1999 for the LMC data). The relationship is also qualitatively similar to that found for O-rich stars (Whitelock et al. 1994 fig. 21) and covers the transition from an optically thin dust shell, $K - [12] < 5$, to optically thick one $K - [12] > 7$.

11 LONG TERM TRENDS, OBSCURATION EVENTS AND THE RCB PHENOMENON

The very extended atmospheres of Miras are intrinsically unstable and all their light curves show some level of vari-

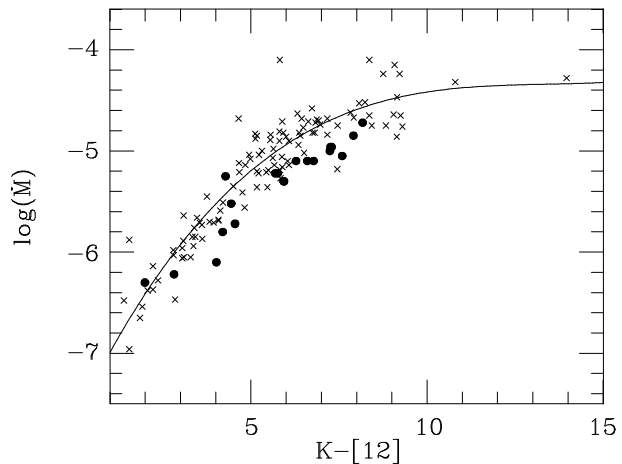


Figure 16. Mass-loss rate as a function of $K - [12]$ colour, for Galactic C Miras (crosses) and LMC C Miras (closed circles, van Loon et al. 1999), the line is equation 12.

ability from one cycle to another. However, some Miras show much greater variability (typically around $\Delta K \sim 1$ mag on top of the normal pulsation), which can be understood as the result of dramatically changing obscuration from dust. Detailed descriptions have been given for R For (Whitelock et al. 1997) and II Lup (Feast et al. 2003) where the obscurations are attributed to the ejection of dust puffs in our line of sight. It is clear from these references that the dust ejection cannot be in the form of a spherically symmetric shell. A similar phenomenon has been noted in the photographic red magnitudes of northern C stars, measured over a period of 30 years (Alksnis 2003).

These obscuration events in C-rich Miras are phenomenologically similar to those observed in the H-deficient RCB C stars. The RCB stars are characterized by apparently random declines in brightness of 7 mag or more in visual light. The brightness variations are a consequence of the ejection of puffs of material at random times and in essentially random directions (e.g. Feast 1996). C-rich dust condensing in these puffs of material is responsible for the observed extinction. There is as yet no consensus on the evolutionary status of, or the mechanism for mass-loss from, RCB stars.

As discussed by Feast et al. (2003) there are differences in the details of obscuration events in Miras and RCB stars, but these are to be expected given the differences in the sizes, outflow velocities and temperatures of the stars involved.

In this section we look at the additional information provided on this phenomenon by the data presented here. The frequency of occurrence is obviously important; we see clear obscuration events in 5 out of 18 Miras for which we have at least 25 observations. This should probably be regarded as a lower limit as some of those with photometry over a limited time may eventually show obscuration events if observed for long enough. We therefore estimate the fraction of C-rich Miras exhibiting obscuration events at very roughly one third. Furthermore, we demonstrated above (see Figs. 8 to 13) that there is no difference in the infrared properties of the Miras in which obscuration events have been observed and those in which they have not. It is therefore

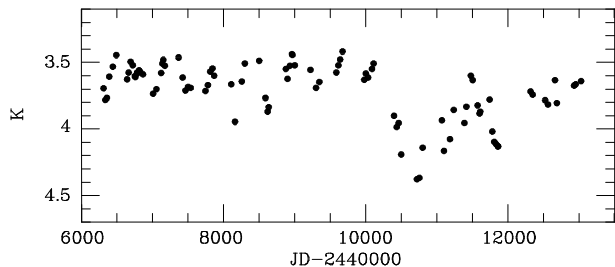


Figure 17. EV Eri at K ; note the obscuration event at around JD 2450700.

possible that all Miras will be seen to do this if monitored for long enough.

Although, as we discuss below, the phenomenon is also observed among non-Miras, the statistics for this group are not reliable. Our primary interest in this work has been the Miras and we generally stopped observing other stars when we had sufficient observations to establish that they were not large amplitude variables.

In the following some individual examples are briefly discussed. Given in brackets after each star name is the variability type (M or SR) and the number of SAAO near-infrared observations that are available. Although more data are presented here we do not reconsider the behaviour of **R For** (M 209) or **II Lup** (M 264) mentioned at the start of this section.

EV Eri (SR 92) was discussed by Whitelock et al. (1997) who estimated its period at 228 days, not significantly different from the 226 days derived here from a slightly larger dataset. Since then it has undergone an obscuration phase (Fig. 17) similar to those shown by the Miras R For (Whitelock et al. 1997) and R Lep (see below and Fig. 18). At its dimmest EV Eri was fainter than usual by $\Delta J \sim 1.1$, $\Delta H \sim 0.9$, $\Delta K \sim 0.8$ and $\Delta L \sim 0.7$ mag. Gigoyan et al. (1998) classified it as C-type (R or N) on an objective prism spectrum and identify it with CGCS611 (Ste85-21), presumably incorrectly as the coordinates differ significantly (EV Eri: 04 09 07.48 -09 14 12.0; CGCS611: 04 03 39.20 -09 13 17.3 (Equinox 2000)). In view of the similarity of the light curve of EV Eri to those of RCB stars it would be interesting to see what a higher resolution spectrum revealed. As discussed above this star shows IRAS colours (see Fig. 2, where $K - [12] = 2.14$ and $[12] - [25] = 1.02$) that are unusual among non-Mira C-rich variables. RCB stars show an excess at near-infrared wavelengths (e.g. Feast et al. 1997; Feast 1997).

R Lep (M 154) was discussed by Whitelock et al. (1997). The light curve from the larger dataset is illustrated in the top part of Fig. 18, while the bottom part shows the K curve after removing the 438 day periodic term (modelled as a sine curve plus its harmonic). The smoothness of this residual is a measure of the regularity of the underlying 438 day pulsation. An analysis of data from the AAVSO archive gives a period of 436 days and shows an earlier deep minimum around JD 2443700 in addition to the one illustrated here.

R Vol (M 88). There is little to add to the discussion by Whitelock et al. (1997), but to note that R Vol is brighter now, at JHK and L than it has ever been in the 24 years we

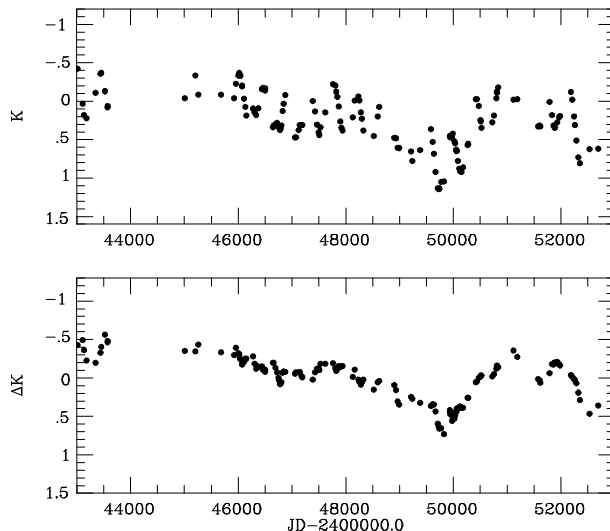


Figure 18. (top) R Lep at K . (bottom) R Lep at K after removal of the 438 day pulsations.

have been observing it. The most recent maximum recorded by the AAVSO, around JD 2453000, is the brightest in almost 100 years. The star may be emerging from a prolonged obscuration event.

09164–5349 (SR 14) has a rather remarkable light curve, illustrated in Fig. 19, which was typical of a very low amplitude SR variable for more than 1000 days before it started a slow decline, changing in brightness by $\Delta K > 2.0$ mag and $\Delta J > 3.5$ mag over the next 800 days. Epchtein et al. (1990) reported $JHKLM$ photometry from January 1986, i.e. almost 10 years before our first observations, at the same bright quiescent level as our early measurements with $K = 2.14$. Because of its unusual IRAS colours (e.g. it lies above the dashed line which separates most O- and C-rich stars in Fig. 2) 09176–5147 has been identified by various authors as a potential C star with silicate dust shell (e.g. Chen et al. 1993) although no evidence was found for anything other than a normal C-rich shell. The colour changes during the fading event suggest an increase in dust absorption. This particular object differs from most others showing dust obscuration events in that it does not show evidence for pulsation or other types of large amplitude variability. Groenewegen et al. (2002) did not detect CO emission.

If 09164–5349 is indeed exhibiting the same type of obscuration event as the other stars discussed in this section it is particularly important because its existence proves that the phenomenon is not necessarily associated with large amplitude pulsation (10136–5743 and 16406–1406 may not be pulsating, but that is not proved beyond any doubt).

10136–5743 (M: 13) has a large amplitude, $\Delta K > 1$ mag, but is not obviously periodic (Fig. 19), although a period of the order of 1000 days is possible if the light curve is erratic. There has been very little published on this object beyond confirmation that it is a carbon star. It may be similar to 16406–1406.

16406–1406 (M: 28) is one of the most peculiar stars in the survey. It is also one of the few objects for which we have no spectroscopic evidence for its C-type classification, and this must therefore be regarded as uncertain.

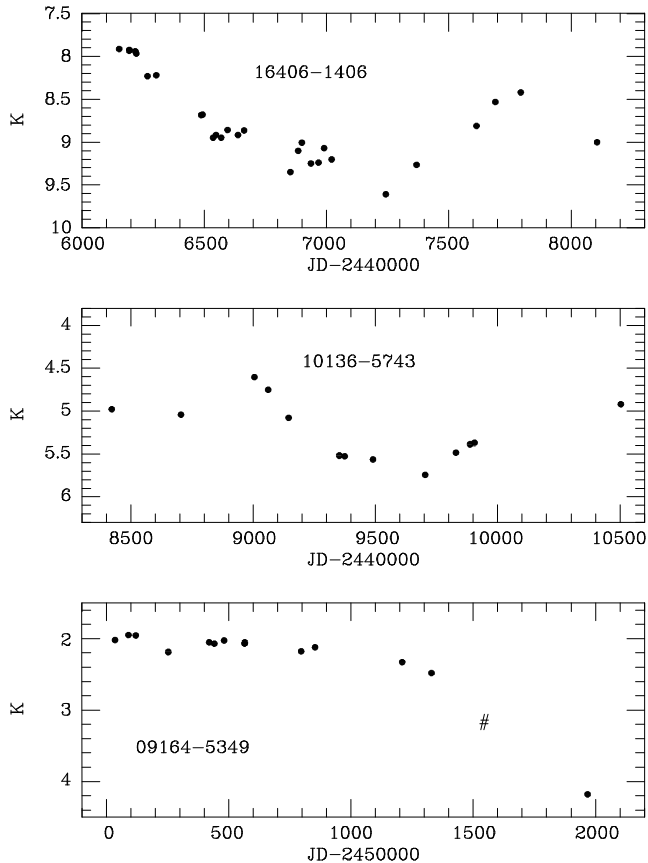


Figure 19. 09176–5147, 10136–5743 and 16406–1406 at K ; the # in the bottom plot is an observation from 2MASS.

There has been very little published about it. Kwok et al. (1997) describe the IRAS spectrum as type-F, i.e. showing a featureless continuum. It is very red $3.3 < K - L < 4.0$, and has large amplitude variations, $\Delta K > 1.5$ mag, with no evidence for periodicity unless it is with a period of about 1800 days and very erratic. Its colours, e.g. $K - [12] = 8.62$ and $[12] - [25] = 0.89$, are certainly typical of a C star with a moderately thick shell. It is in the Galactic Centre quadrant, but well out of the Galactic plane ($\ell = 4.1$, $b = 20.2$).

16406–1406 has similarities to 10136–5743. It is also possible that it is like R For and that the periodicity has been totally disrupted by an obscuration event. In Table 2 we tentatively classified it as a Mira because of its large amplitude variability, but the light curve of Fig. 19 does not suggest Mira-like periodicity.

In summary, these obscuration events occur in very roughly one third of C-rich Miras and in an unknown fraction of other C-rich variable stars. It is possible that they are related to the RCB phenomenon as discussed above and it would certainly be worth making a more detailed study of the abundances and other properties of these stars. It is also possible that these stars are in binary systems with low level interactions. It may even be that the RCB-like mass loss is triggered by binary-related effects. Although obscuration events are not seen among solitary O-rich Miras they are very common among symbiotic Miras (Whitelock 1987), where they are thought to be a consequence of binary star interaction. It is also worth noting that the well studied C-

rich binary SR variable V Hya shows colour changes (e.g. Olivier et al. 2001) which are modulated at its orbital period but which otherwise look very similar to the obscuration phenomenon under discussion. At the same time we do have enough data to be certain that the obscuration events in R For are not periodic (Whitelock et al. 1997).

Finally we note that Woitke & Niccolini’s (2005) results offer at least a partial explanation of the obscuration events. In their model for dust driven winds in AGB stars, instabilities (hydrodynamical, radiative or thermal) allow the occasional formation of dust clouds close to the star in temporarily shielded areas; these clouds are then accelerated outward by radiation pressure. At the same time, but elsewhere, thinner dust-free matter falls back towards the star. In this way a turbulent and dynamical environment is created close to the star, which can be expected to produce the strongly inhomogeneous dust distribution which we observe in the C stars discussed here.

ACKNOWLEDGMENTS

We thank the following people for their contribution to the SAAO observations reported here: Brian Carter, Robin Catchpole, Ian Glass, Dave Laney, Lerethodi Leeuw, Karen Pollard, Greg Roberts, Jonathan Spencer-Jones, Garry Van Vuren, Hartmut Winkler and Albert Zijlstra. We are grateful to Tom Lloyd Evans, Steven Bagnulo and Ian Short for allowing us to use their data in advance of publication. We also thank Luis Balona for the use of his STAR Fourier analysis package and John Menzies for a critical reading of the manuscript. This research has made use of the SIMBAD database, operated at CDS, Strasbourg, France. We acknowledge with thanks the variable star observations from the AAVSO International Database contributed by observers worldwide and used in this research. We are grateful to the referee, Jacco van Loon for some helpful suggestions.

REFERENCES

- Aaronson M., Blanco V. M., Cook K. H., Schechter P. L., 1989, *ApJS*, 70, 637
- Alksnis A., 2003, *Baltic Astron.*, 12, 595
- Alksnis A., Balklavs A., Dzervitis U., Eglitis I., Paupers O., Pundure I., 2001, *Balt. A.*, 10, 1
- Bujarrabal V., Cernicharo J., 1994, *A&A*, 288, 551
- Bateson F., McIntosh R., Venimore C. W., 1988, *RASNZ Publ. Var. Star Sec.*, 15, 70
- Bergeat J., Knapik A., Rutily B., 1998, *A&A*, 332, L53
- Bergeat J., Knapik A., Rutily B., 2002, *A&A*, 390, 967
- Bergeat J., Chevallier L., 2005, *A&A*, 429, 235
- Carter B. S., 1990, *MNRAS*, 242, 1
- Catchpole R. M., Feast M. W., 1976, *MNRAS*, 175, 501
- Catchpole R. M., Robertson B. S. C., Lloyd Evans T. H. H., Feast M. W., Glass I. S., Carter B. S., 1979, *SAAO Circ.*, 1, 61
- Chen P.-S., Lou E.-R., Li J.-Q., 1993, *Acta Astron. Sinica*, 34, 92
- Chen P. S., Zhang P., Fu H. W., 2003, *New Astron.*, 8, 719
- Cutri R. M., 2003, “The 2MASS All-Sky Catalog of Point Sources”, IPAC/CIT (2MASS)
- Cohen J. G., Frogel J. A., Persson S. E., Elias J. H., 1981, *ApJ*, 249, 481
- Drimmel R., Cabrera-Levers A., López-Corredoira M., 2003, *A&A*, 409, 205

- Egan M. P., Price S. D., Kraemer K. E., Mizuno D. R., Carey S. J., Wright C. O., Engelke C. W., Cohen M., Gugliotti G. M., 2003, Air Force Research Laboratory Technical Report AFRL-VS-TR-2003-1589
- Epchtein N., Le Bertre T., Lépine J. R. D., 1990, *A&A*, 82, 104
- ESA 1997, The Hipparcos and Tycho Catalogues, ESA SP-1200
- Feast M. W., 1954, *Mem. Soc. R. Sci. Liège*, 14, 413
- Feast M. W., 1996, in: S. Jeffrey, U. Heber (eds.), *Hydrogen Deficient Stars and Related Objects*, ASP Conf. Ser. 96, p. 3
- Feast M. W., 1997, *MNRAS*, 285, 339
- Feast M. W., Whitelock P. A., 2000, in: F. Matteucci, F. Giovannelli (eds.) *The Evolution of the Milky Way: stars versus clusters*, Kluwer Academic Publishers, Dordrecht, ISBN 0-7923-6679-4, p. 229
- Feast M. W., Whitelock P. A., Catchpole R. M., Roberts G., Carter B. S., 1985, *MNRAS*, 215, 63P
- Feast M. W., Glass I. S., Whitelock P. A., Catchpole R. M., 1989, *MNRAS*, 241, 375
- Feast M. W., Carter M. S., Roberts G., Marang F., Catchpole R. M., 1997, *MNRAS*, 285, 317
- Feast M. W., Whitelock P. A., Marang F. 2003, *MNRAS*, 346, 878
- Feast M. W., Whitelock P. A., Menzies J. W., 2006, *MNRAS*, submitted (Paper III)
- Fouqué P., Le Bertre T., Epchtein N., Guglielmo F., Kerschbaum F., 1992, *A&AS*, 93, 151
- Gaylard M. J., Whitelock P. A., 1988, *MNRAS*, 235, 123
- Gaylard M. J., West M. E., Whitelock P. A., Cohen R. J., 1989, *MNRAS*, 236, 247
- Gezari D. Y., Pitts P. S., Schmitz M., 1997, *Catalog of Infrared Observations*, Edition 4, unpublished 1997
- Gigoyan K. S., Hambaryan V. V., Azzopardi M., 1998, *Astrophys.*, 41, 356
- Glass I. S., 1999, *Handbook of Infrared Photometry*, CUP
- Glass I. S., Lloyd Evans T., 2003, *MNRAS*, 343, 67
- Groenewegen M. A. T., 1994, *A&A*, 290, 207
- Groenewegen M. A. T., Whitelock P. A., 1996, *MNRAS*, 281, 1347
- Groenewegen M. A. T., de Jong T., Baas F., 1993, *A&AS*, 101, 513
- Groenewegen M. A. T., Whitelock P. A., Smith C. H., Kerschbaum F., 1998, *MNRAS*, 293, 18
- Groenewegen M. A. T., Sevenster M., Spoon H. W. W., Pérez I., 2002, *A&A*, 390, 511
- Guandalini R., Busso M., Ciprini S., Silvestro G., Persi P., 2005, *astro-ph/0509739*
- Guglielmo F., Epchtein N., Le Bertre T., Fouqué P., Hron J., Kerschbaum F., Lépine J. R. D., 1993, *A&AS*, 99, 31
- Iben I., Jr, 1981, *ApJ*, 246, 278
- IRAS Science Team, 1988, *Explanatory Supplement to the IRAS Point Source Catalogue*
- Jones T. J., Bryja C. O., Gehrz R. D., Harrison T. E., Johnson J. J., Klebe D. I., Lawrence G. F., 1990, *ApJS*, 74, 785
- Jura M., 1987, *ApJ*, 313, 743
- Keenan P. C., Boeshaar P. C., 1980, *ApJS*, 43, 379
- Knapik A., Bergeat J., Rutily B., 1998, *A&A*, 334, 545
- Kwok S., Volk K., Bidelman W. P., 1997, *ApJS*, 112, 557
- Le Bertre T., 1992, *A&AS*, 94, 377
- Le Bertre T., Matsuura M., Winters J. M., Murakami, H., Yamamura I., Freund M., Tanaka M., 2001, *A&A*, 376, 997
- Lloyd Evans T., 1991, *MNRAS*, 249, 409
- Lloyd Evans T., 1997, *MNRAS*, 286, 839
- Lloyd Evans T., Catchpole R. M., 1989, *MNRAS*, 237, 219
- Luyten W. J., 1927, *HB No.842*, 9
- Maffei P., 1966, *Mem. Soc. Ast. It.*, 37, 475
- Matsuura M., Zijlstra A. A., van Loon J. Th., Yamamura I., Markwick A. J., Whitelock P. A., Woods P. M., Marshall J. R., Feast M. W., Waters L. B. F. M., 2005, *A&A*, 436, 691
- Menzies J., Feast M., Tanabé T., Whitelock P., Nakada Y., 2002, *MNRAS*, 335, 923
- Menzies J. W., Feast M. W., Whitelock P. A., 2006, *MNRAS*, submitted (Paper II)
- Moshir M. et al. 1989, *IRAS Faint Source Catalog, Version 2, Infrared Processing and Analysis Centre*
- Noguchi K., Kawara K., Kobayashi Y., Okuda H., Sato S., Oishi M., 1981, *PASJ*, 33, 373
- Olivier E. A., Whitelock P. A., Marang F., 2001, *MNRAS*, 326, 490
- Ortiz R., Lorenz-Martins S., Maciel W. J., Rangel E. M., 2005, *A&A*, 431, 565
- Pojmański G., 2002, *Acta. Astron.*, 52, 397 (www.astro.uw.edu.pl/~gp/asas/asas.html)
- Richichi A., Stecklum B., Herbst T. M., Lagage P.-O., Thamm E., 1998, *A&A*, 334, 585
- Samus N.N., Durlevich O.V., et al., 2004, "Combined General Catalog of Variable Stars" (GCVS4.2, 2004 Ed.) Moscow, Institute of Astronomy of Russian Academy of Sciences (GCVS)
- Skinner C. J., Griffin I., Whitmore B., 1990, *MNRAS*, 243, 78
- Stancliffe R. J., Izzard, R. G., Tout C. A., 2005, *MNRAS*, 356, L1
- Tuthill P. G., Monnier J. D., Danchi W. C., Lopez B., 2000, *ApJ*, 243, 284
- van Leeuwen F., Fantino E., 2005, *A&A*, 439, 791
- van Leeuwen F., 2005, *A&A*, 439, 805
- van Loon J. Th., 2006, in: (eds.) Lamers, Langer, Nugis & Annuk, *Stellar Evolution at Low Metallicity: Mass Loss, Explosions, Cosmology*, ASP, in press astro-ph/0512326)
- van Loon J. Th., Groenewegen M. A. T., de Koter A., Trams N. R., Waters L. B. F. M., Zijlstra A. A., Whitelock P. A., Loup C., 1999, *A&A*, 351, 559
- Walker W. S. G., Ives F. V., Williams H. O., 1995, *Southern Stars*, 36, 123
- Whitelock P. A., 1987, *PASP*, 99, 573
- Whitelock P. A., Feast M. W., 2000, *MNRAS*, 319, 759
- Whitelock P. A., Pottasch, S. R., Feast, M. W., 1987, in: (eds.) S. Kwok & S. R. Pottasch, *Late Stages of Stellar Evolution*, Reidel, Dordrecht, p. 269
- Whitelock P. A., Menzies J.W., Feast M.W., Marang F., Carter B., Roberts G., Catchpole R. M., Chapman J., 1994, *MNRAS*, 267, 711
- Whitelock P. A., Menzies J.W., Feast M.W., Catchpole R.M., Marang F., Carter B., 1995, *MNRAS*, 276, 219
- Whitelock P. A., Feast M.W., Marang F., Overbeek M.D. 1997, *MNRAS*, 288, 512
- Whitelock P. A., Marang F., Feast M. W. 2000, *MNRAS*, 319, 728
- Whitelock P. A., Feast M. W., van Loon, J. Th., Zijlstra, A. A., 2003, *MNRAS*, 342, 86
- Woitke P., Niccolini G., 2005, *A&A*, 433, 1101
- Young K., Phillips T. G., Knapp G. R., 1993, *ApJS*, 86, 517
- Zijlstra A. A., Bedding T. R., Markwick A. J., Loidl-Gautschy R., Tabur, V., Alexander K. D., Jacob, A. P., Kiss L. L., Price A., Matsuura M., Mattei J. A., 2004, *MNRAS*, 352, 325

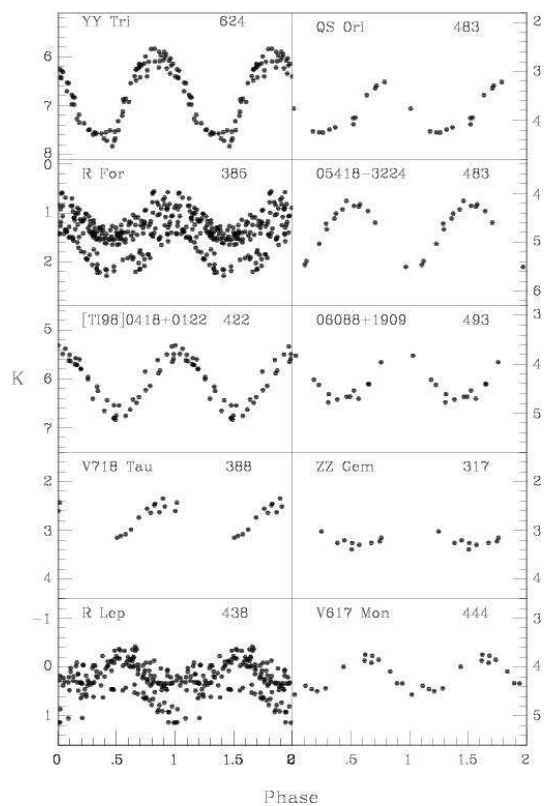


Figure A-1. *K* light curves for the Mira variables; each point is plotted twice to emphasize the periodicity.

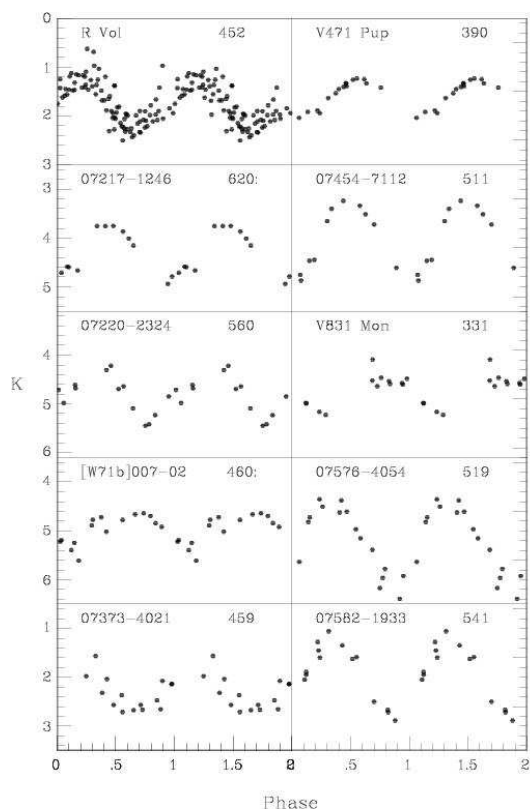


Figure A-1. continued *K* Mira light curves.

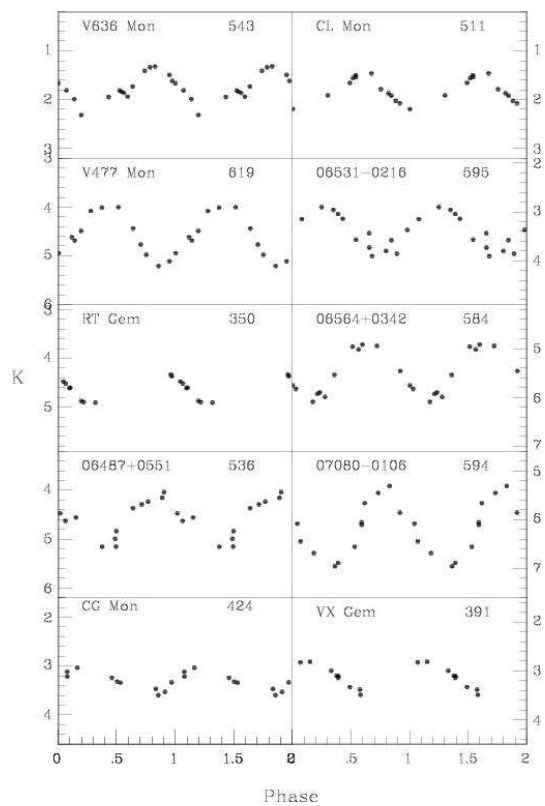


Figure A-1. continued *K* Mira light curves.

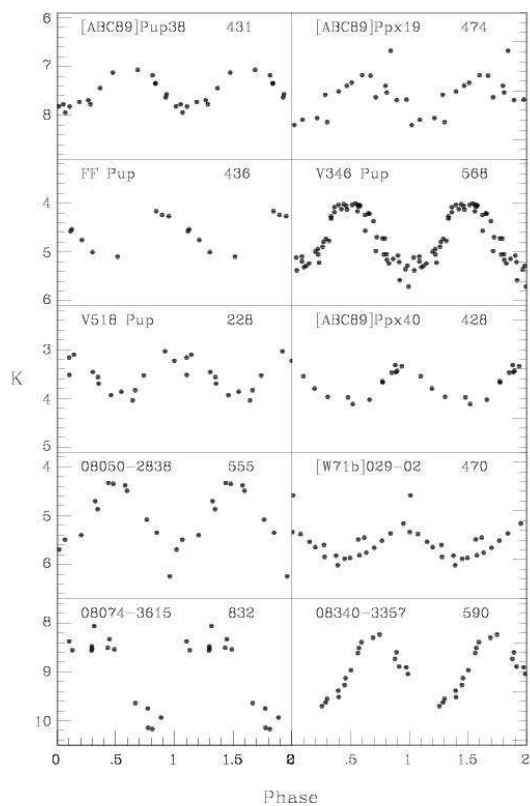


Figure A-1. continued *K* Mira light curves.

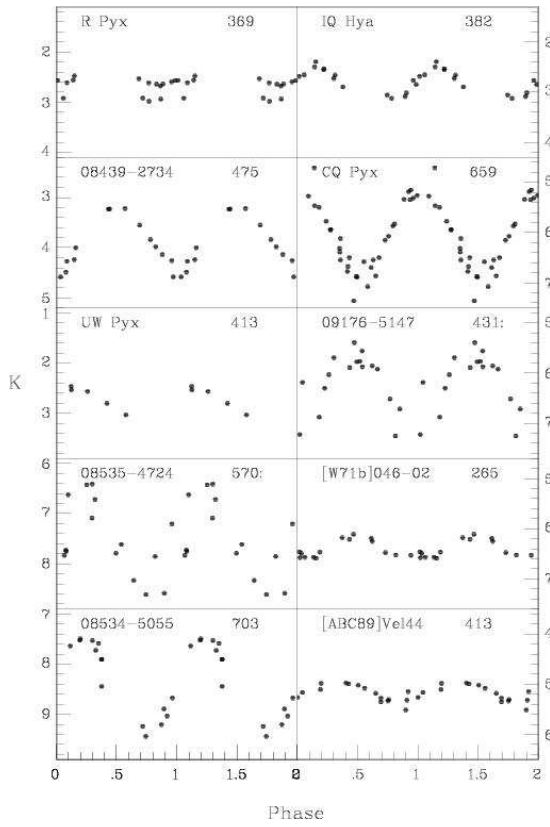


Figure A-1. continued *K* Mira light curves.

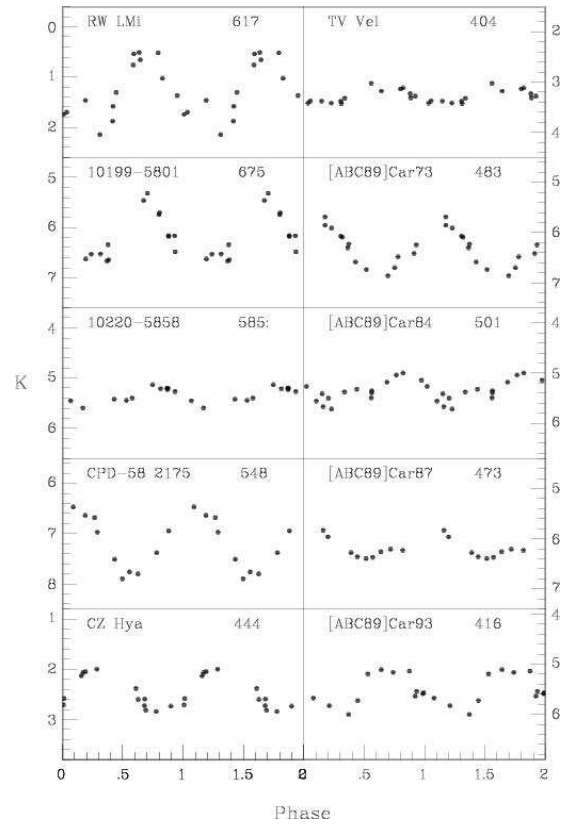


Figure A-1. continued *K* Mira light curves.

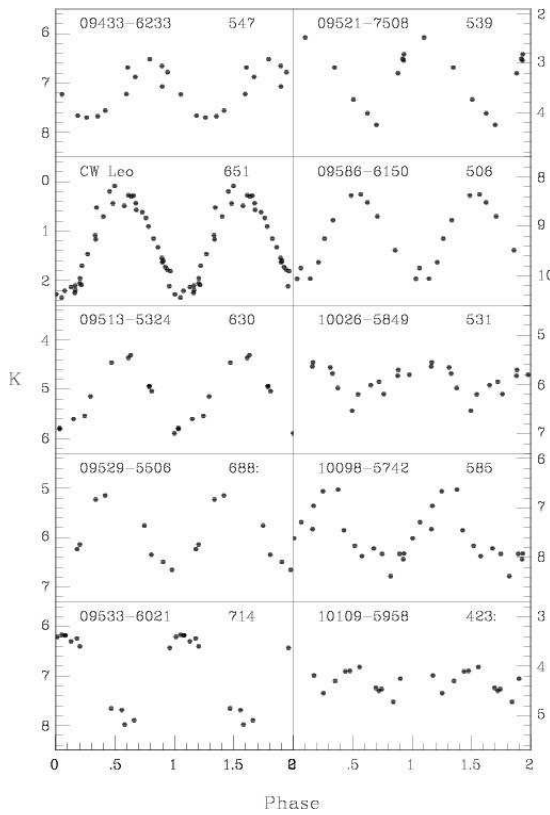


Figure A-1. continued *K* Mira light curves.

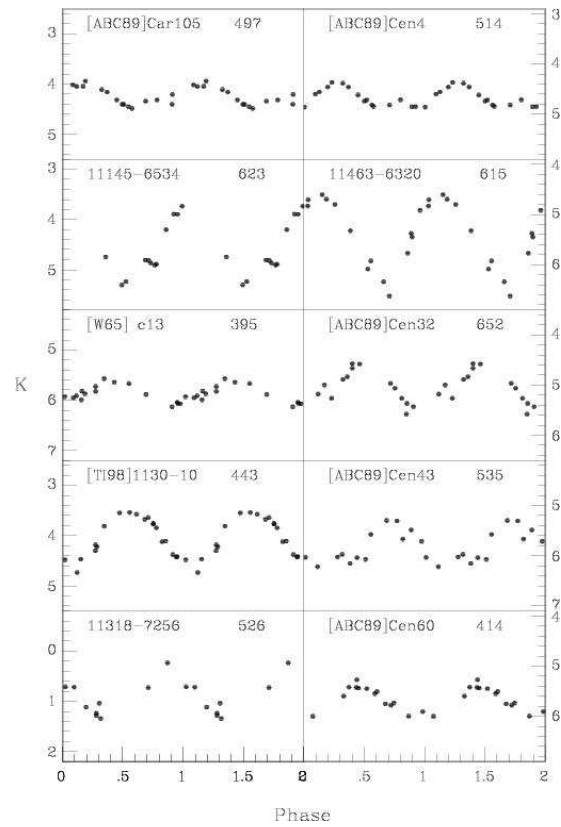


Figure A-1. continued *K* Mira light curves.

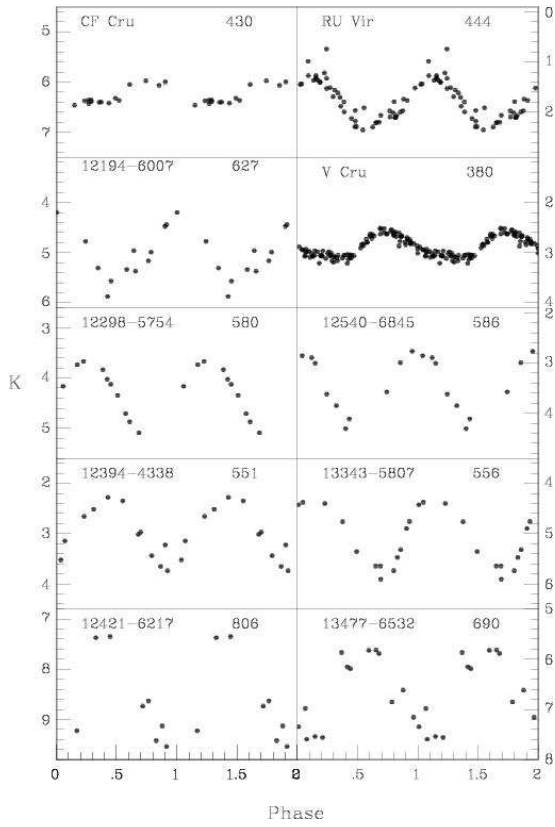


Figure A-1. continued *K* Mira light curves.

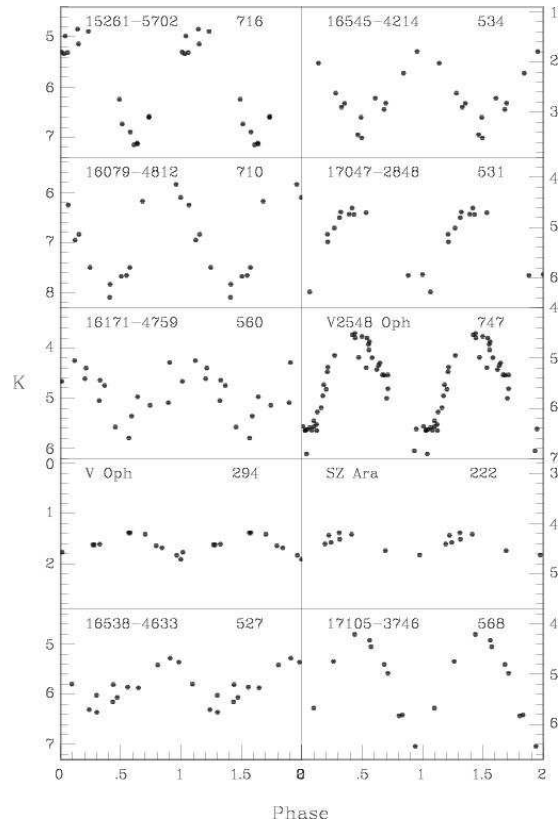


Figure A-1. continued *K* Mira light curves.

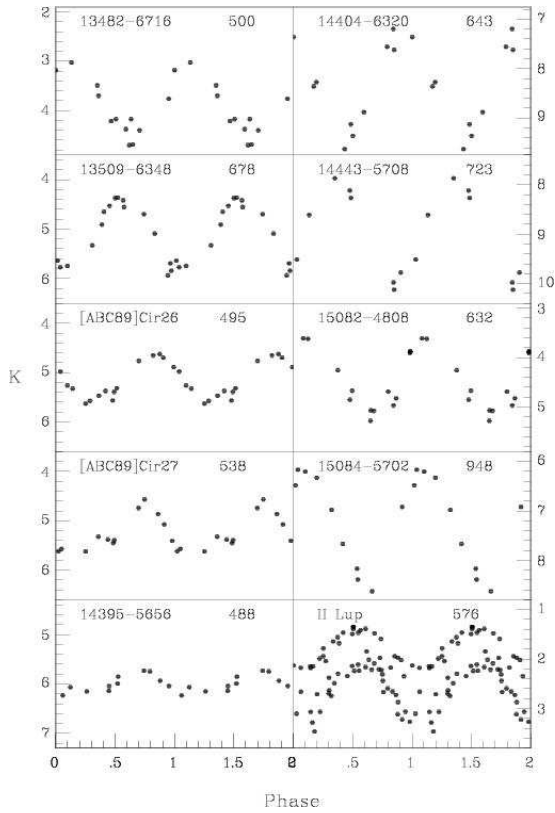


Figure A-1. continued *K* Mira light curves.

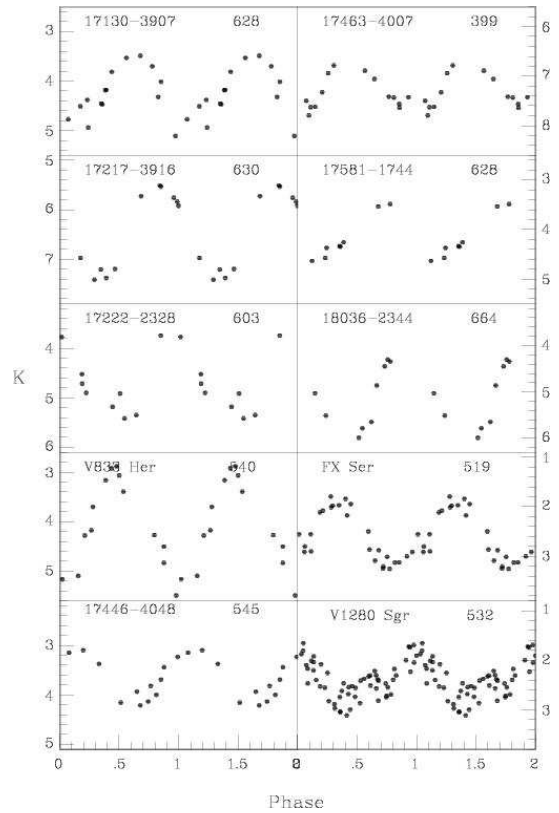


Figure A-1. continued *K* Mira light curves. The curve for V833 Her extends beyond the range shown here.

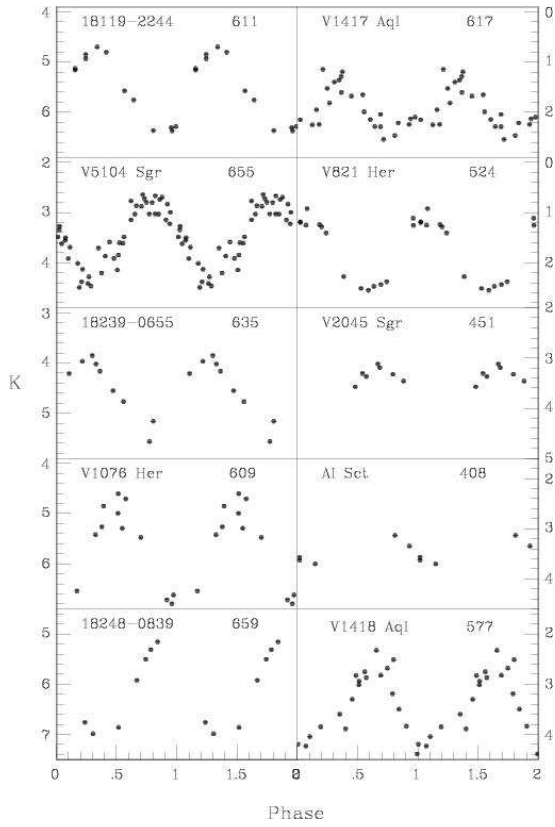


Figure A-1. continued *K* Mira light curves.

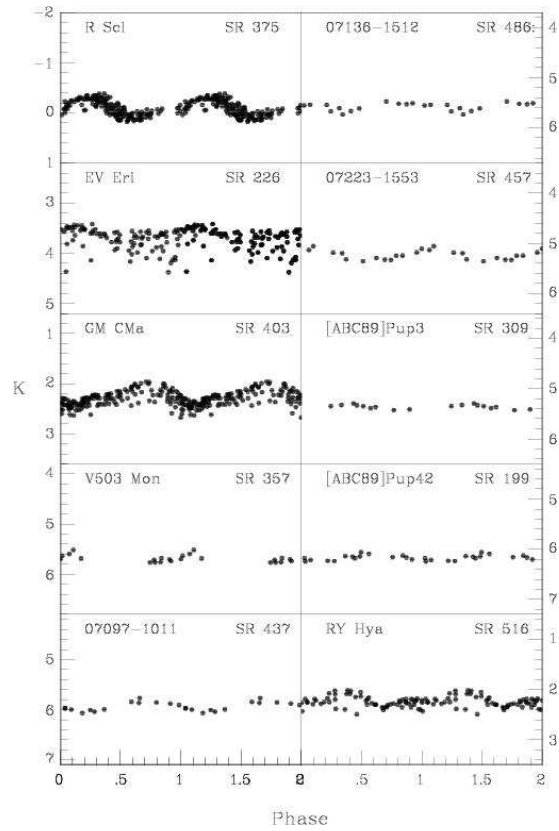


Figure A-2. *K* light curves for semi-regular variables on the same scale as the Miras.

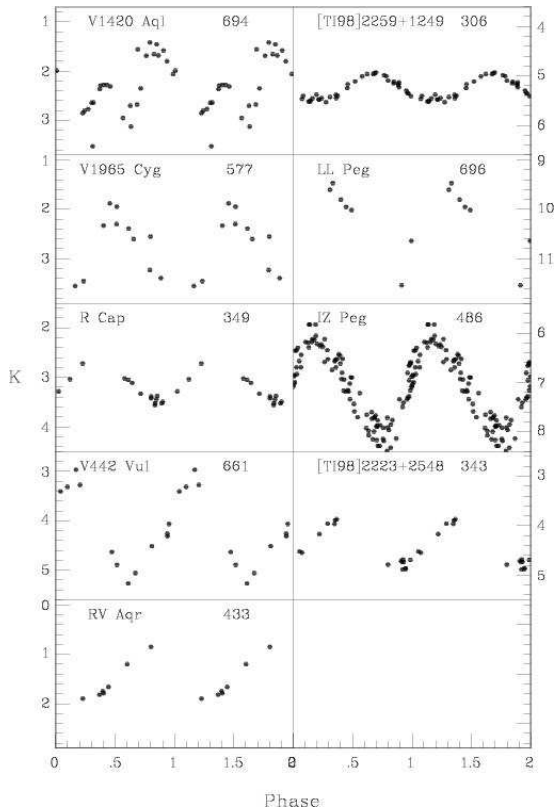


Figure A-1. continued *K* Mira light curves.

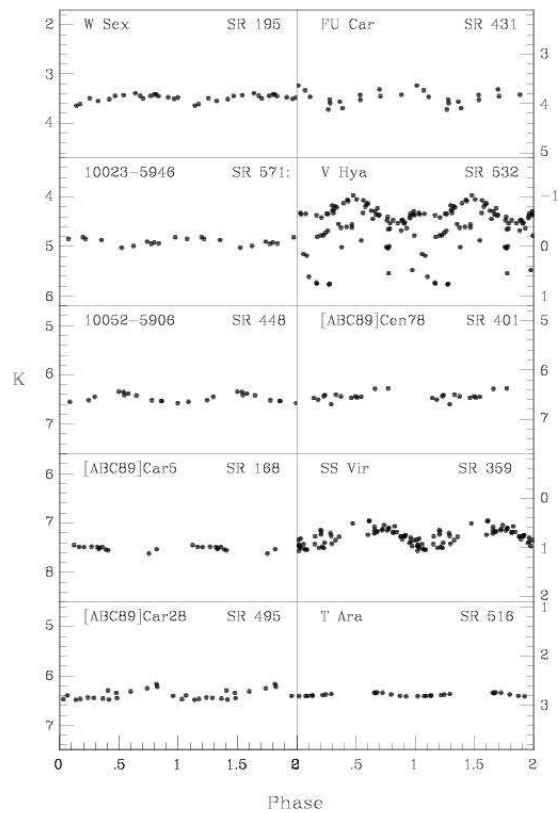


Figure A-2. continued *K* SR light curves.

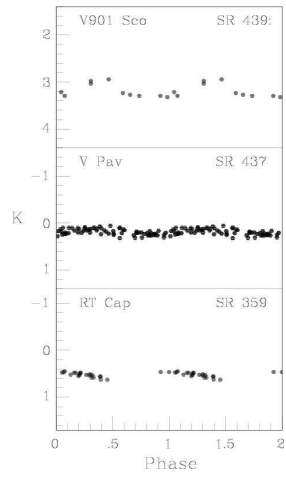


Figure A-2. continued *K* SR light curves.